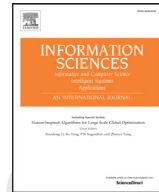




Contents lists available at ScienceDirect

Information Sciences

journal homepage: www.elsevier.com/locate/ins

A novel adaptive hybrid crossover operator for multiobjective evolutionary algorithm

Q1 Qingling Zhu, Qiuzhen Lin*, Zhihua Du, Zhengping Liang, Wenjun Wang,
Zexuan Zhu, Jianyong Chen, Peizhi Huang, Zhong Ming

College of Computer Science and Software Engineering, Shenzhen University, Shenzhen, PR China

ARTICLE INFO**Article history:**

Received 4 July 2015

Revised 8 December 2015

Accepted 22 January 2016

Available online xxx

Keywords:

Evolutionary algorithm
Multiobjective optimization
Simulated binary crossover
Differential evolution

ABSTRACT

In this paper, a novel recombination operator, called adaptive hybrid crossover operator (AHX), is designed for tackling continuous multiobjective optimization problems (MOPs), which works effectively to enhance the search capability of multiobjective evolutionary algorithms (MOEAs). Different from the existing hybrid operators that are commonly operated on chromosome level, the proposed operator is executed on gene level to combine the advantages of simulated binary crossover (SBX) with local search ability and differential evolution (DE) with strong global search capability. More opportunities are assigned to DE in the early evolutionary stage for gene-level global search in decision space; whereas, with the generation grows, more chances are gradually allocated to SBX for gene-level local search. The balance between the gene-level global and local search is well maintained by an adaptive control approach in AHX. To validate the effectiveness of AHX, it is studied by substituting the original recombination operators in the four state-of-the-art MOEAs (i.e., NSGA-II, SPEA2, SMS-EMOA, and MOEA/D), and the performance of revised algorithms is significantly improved. Furthermore, AHX is also compared to three recently proposed recombination operators, such as a newly DE inspired (DEI) recombination operator, a learning paradigm based on jumping genes (JGBL) and a bandit-based adaptive operator selection approach (FRRMAB). The experimental studies validate that AHX can be effectively integrated into different frameworks of MOEAs, and performs better than SBX, DE, DEI, JGBL and FRRMAB in solving various kinds of MOPs.

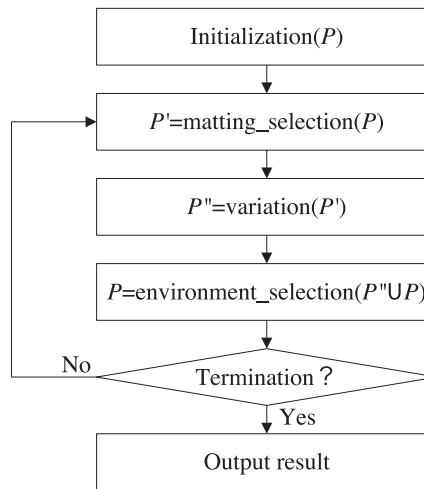
© 2016 Published by Elsevier Inc.

1. Introduction

In the past several decades, various kinds of evolutionary algorithms (EAs) have been proposed to solve optimization problems, which are modeled from many scientific and application fields, such as science, economic and engineering [1,53,66]. Based on the inspired evolutionary mechanisms, EAs can be classified into the following categories, such as genetic algorithms (GAs) [13,24], evolutionary strategies (ESs) [2,29], genetic programming (GP) [27,28], evolutionary programming (EP) [5,17], and other nature-inspired algorithms [4,7,18,51,52,56]. Among the existing EAs, GAs are widely recognized as the most popular and commonly used optimization algorithms, which have been applied in many engineering applications [30,48,49]. Naturally, as a kind of population-based random search approach, GAs mimic the natural selection principle "survival of the fittest" from the biological world. In the early study of GAs, the candidate solutions are mostly encoded by

* Corresponding author. Tel.: +86 75526001223; fax: +86 75526534078.

E-mail addresses: zhuqingling@email.szu.edu.cn (Q. Zhu), qiuzhlin@szu.edu.cn, qiuzhlin@qq.com (Q. Lin).

**Fig. 1.** A general framework of MOEAs.

10 the binary values to simulate the chromosome [23,50]. However, when tackling the optimization problems with continuous
 11 search space, the real-coded approach is found to be more suitable for the representation, where a chromosome in GAs is
 12 expressed by a vector of real numbers [13,55].

13 When dealing with multiobjective optimization problems (MOPs), evolutionary algorithms have been recognized to be
 14 effective and efficient due to their population-based property to obtain an approximation of the Pareto-optimal set in a
 15 single run. Since the pioneering work of Schaffer [50], numerous multiobjective evolutionary algorithms (MOEAs) have been
 16 proposed. Based on the used type of selection mechanism, most of MOEAs can be classified into the following three cate-
 17 gories: Pareto-based approaches [13,69], indicator-based approaches [3,35,68], and decomposition-based approaches [38–40].
 18 The Pareto-based methods incorporate the Pareto optimality into the selection process. The representative of this category
 19 includes NSGA-II [13] and SPEA2 [69]. They are further extended to solve many-objective optimization problems (more than
 20 3 objectives) by revising the environment selection method, named NSGA-III [12] and SPEA2-SDE [32]. The indicator-based
 21 approaches integrate the convergence and diversity into a single indicator, such as hyper-volume [70], to guide the selec-
 22 tion process. The representative of this category includes IBEA [68] and SMS-EMOA [3]. The decomposition-based techniques
 23 decompose a MOP into a set of sub-problems and optimize them in a collaborative manner. The representative of this cat-
 24 egory includes MOEA/D [40] and MOEA/D-STM [39]. Recently, some interesting approaches are designed to combine the
 25 Pareto-based and decomposition-based methods, such as ND/DDP [36] and NSGA-III [12].

26 In general, there are essentially three fundamental evolutionary operators in MOEAs, i.e., selection, crossover and mu-
 27 tation, which are employed to gradually approach the optimal solution. The selection operator usually has two aspects,
 28 including matting selection and environment selection [69]. Matting selection is aimed at picking out the better-fit chromo-
 29 somes, which are evolved by the variation operators such as crossover and mutation. Crossover operator exchanges the gene
 30 information of the parents, in order to share the better gene segment. After that, mutation operator randomly alters some
 31 genes of the chromosome to perform a local search, attempting to find better fitness landscape. At last, the environment
 32 selection operator determines the survived population for the next generation, which is usually selected from the union
 33 population of parents and their offspring. This general framework of MOEAs is illustrated in Fig. 1, where the variation
 34 operators include crossover and mutation operators.

35 Considering the crossover operator, many research works have been conducted on improving the performance. This is
 36 because crossover is a very important evolutionary procedure in the three fundamental operators as justified in [6,41–
 37 45,47,54,61]. According to the expected position of the offspring distributed in solution space, most of the existing
 38 crossover operators can be generally classified into two kinds: parent-centric crossover [10,11,15] and mean-centric crossover
 39 [22,43,59]. However, the quality of the offspring produced by the parent-centric crossover or mean-centric crossover is
 40 highly dependent on the characteristics of target problems, which in turn means that different crossover operators may
 41 behave diversely in solving various kinds of optimization problems. Thus, multiple crossover operators are combined, which
 42 can repair the weakness of a single crossover operator and is able to deal with various types of optimization problems [62].

43 These existing hybrid crossover approaches [31,44,45,47,57,63] have been experimentally validated to perform better than
 44 the single use of one crossover operator, especially in solving some complicated optimization problems. In these schemes, a
 45 child population is built by using different crossover operators, and a child solution is derived by certain selected crossover
 46 operator. That is to say, all genes of child chromosome are inherited from the parents using the same recombination man-
 47 nner, which may not provide sufficient diversity in child chromosome. Therefore, in this paper, we propose a novel adaptive
 48 hybrid crossover (AHX) method, attempting to produce each gene of child chromosome using different crossover operators.
 49 By this way, AHX is essentially a gene-level hybrid crossover operator. In our scheme, a parent-centric crossover operator

SBX is adopted to generate exploitation gene, while a DE crossover is employed to produce exploration gene. Thus, one chromosome using AHX can simultaneously have exploitation gene and exploration gene. The balance between the exploitation and exploration during the evolutionary phase is well managed by the proposed adaptive control approach. Our proposed AHX operator is designed to have a fast convergence speed and good population diversity. Although a novel recombination operator (named DEI) has been studied in [45] to combine the SBX and DE operators, two significant differences about our AHX and DEI are clarified here. One difference is that DEI is a chromosome-level hybrid recombination operator while AHX is a gene-level hybrid recombination operator. In other words, every gene of a chromosome in DEI is generated by using the same crossover principle (SBX or DE), while each gene of a chromosome in AHX can be obtained by either using SBX crossover or DE crossover. The other difference is that the static parameter settings are employed in DEI, while an adaptive parameter control approach is designed in AHX. The above differences enable AHX to significantly outperform DEI, which are also validated by the experimental studies. To investigate the performance of AHX, 31 well-known benchmark problems such as ZDT problems [67], WFG problems [25], DTLZ problems [14], and UF problems [64] are adopted. When using our proposed AHX operator to replace the original crossover operator (SBX and DE) in the frameworks of NSGA-II [13], SPEA2 [69], SMS-EMOA [3] and MOEA/D [40], the performance of correspondingly revised algorithms is substantially enhanced. Moreover, AHX is also experimentally validated to outperform three newly proposed hybrid crossover operators [37,34,45], when it is implemented in IMADE [45] to compare with the DEI operator, in SPEA2 to compare with JGBL [37], and in MOEA/D to compare with FRRMAB [34]. These experimental results validate the advantage of the proposed AHX operator.

The rest of this paper is organized as follows. The related work and motivation of this paper are introduced in Section 2, while the proposed AHX operator and the corresponding adaptive control approach are detailedly described in Section 3. Section 4 gives the experimental studies, where the proposed AHX operator is compared with the state-of-the-art crossover operators (i.e., SBX and DE) and three newly proposed hybrid crossover operators (i.e., DEI, JGBL and FRRMAB). At last, the conclusions and future works are summarized in Section 5.

2. Related work and motivation

In this section, we give a review on the existing crossover operators in Section 2.1, where three kinds of crossover operators are introduced. Due to the fact that the existing crossover operators are all operated on chromosome level, the motivation of this paper is clarified in Section 2.2, to point out that the proposed AHX operator is a novel gene-level crossover operator with the enhanced search ability.

2.1. Existing crossover operators

Crossover operator usually inherits the genetic information of two or more parents in order to find a better child solution. This is based on the biological phenomenon that the exchange of genes between good chromosomes has high probability to produce a better child chromosome. As described in Section 1, most of the existing crossover operators can be classified into parent-centric crossover and mean-centric crossover according to the distribution of offspring in search region.

The parent-centric crossover steers the evolutionary search to the surrounding regions of the parents, such as simulated binary crossover (SBX) [10], Laplace crossover (LX) [15] and parent central crossover (PCX) [11]. SBX generates two child solutions from two parent solutions. By simulating the principle of single point crossover in binary coded string, SBX has more opportunities to sample child solutions near to their parent solutions, in which the children's position is determined following a polynomial probability distribution. LX performs similarly with SBX, except that it employs the Laplace distribution as the density function to decide the children's position. An improved version of LX operator, named bounded exponential crossover (BEX), was proposed by Thakur et al. [58], which always creates child solutions bounded within the limit of decision variables. PCX gives a high probability to produce a solution close to each parent, rather than around the center of the parents.

The mean-centric crossover drives the evolutionary search to the mean center of the parents' position, including blend crossover (BLX- α) [22], uni-modal normal distribution crossover (UNDX) [43], and simplex crossover (SPX) [59]. BLX- α was proposed by Eshelman and Schaffer [22] based on the concept of interval schema. The parameter α controls the position of the child solution generated by parent solutions. Their experimental results show that $\alpha = 0.5$ gives the best performance for BLX- α , which indicates that BLX- α prefers to generate child solutions near to the center of two parent solutions [6,57]. UNDX can obtain two or more child solutions from three parent chromosomes based on the ellipsoidal probability distribution [43]. Basically, the UNDX operator gets a high probability to sample child solutions near to the center of first two parents, and a considerably low probability to create solutions near to the parents. SPX produces child solutions by a simplex formed by three or more parent chromosomes, which is experimentally found to be more suitable for solving multi-modal optimization problems [6,57].

Beside the above parent-centric and mean-centric crossover operators, differential evolution (DE) operator proposed by Storn and Price [56] is found to have a strong global search ability when it is used as a crossover operator to solve various optimization problems [8,20,21,34,41,65]. For example, in [20], a new multi-parent crossover (MPC) was presented, which generates three child solutions by using basic DE with different difference vectors from three parents. Its performance was further validated by tackling a wider range of optimization problems [21]. In MOEA/D-DE [40], DE operator was employed to replace the SBX operator in the framework of decomposition-based multiobjective evolutionary algorithm (MOEA/D) [65].

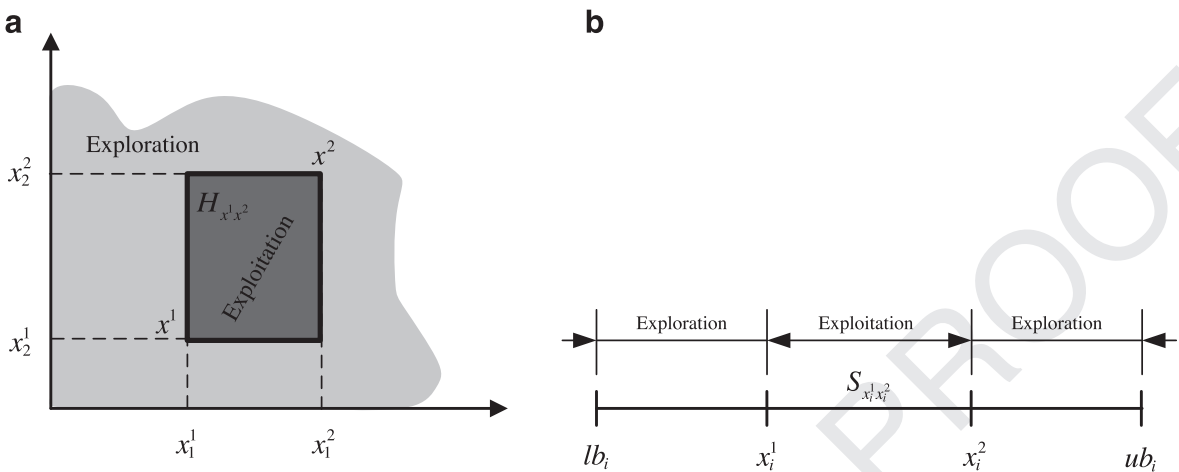


Fig. 2. (a) Hypercube encircled by two genes of parents; (b) Representation of the segment defined by the i th genes of two chromosomes.

107 An improved version of MOEA/D-DE, called MOEA/D-FRRMAB [34], was designed by using a new bandit-based adaptive
 108 operator selection method to adaptively select one DE operator from four different DE candidates. A new multiobjective
 109 DE algorithm was proposed by running two adaptive mechanisms in parallel [33]. In this approach, an adaptive operator
 110 selection mechanism is used to control which DE operator is applied at each instant of the search and an adaptive parameter
 111 control method is employed to adjust the parameter settings of DE operators. A novel adaptive DE method for solving
 112 multiobjective optimization problems was also designed by us [41]. In this approach, it utilizes the global search ability of
 113 DE to compensate the lack of diversity for immune algorithm.

114 Recently, various types of hybrid crossover operators have been developed to analyze the synergy by combining differ-
 115 ent types of crossover operators. Ripon et al. [47] proposed a real-coded jumping gene genetic algorithm (RJGGA), in which
 116 a jumping gene operator combining polynomial mutation and SBX operator is introduced. An improved version of RJGGA,
 117 named JGBL, was proposed by Li et al. [37]. This work adopts the jumping genes operation to enhance the exploration ability
 118 of EMO search. In particular, this operation can be used in an implicitly adaptive manner. Yu et al. [63] presented a mixed
 119 crossover strategy, which blends multiple crossover operators, such as two-point crossover, uniform crossover and arith-
 120 metic crossover. In [44], Pant et al. introduced a modified version of the original DE called DEPCX. This approach integrates
 121 a parent centric approach PCX [11] and DE operator to generate child population. In [31], Li et al. designed a novel variation
 122 operator, called segment-based search (SBS). In this approach, SBS is only activated when the number of non-dominated
 123 solutions exceeds the archive size. The exceeded parts of non-dominated solutions are then executed by SBS while archive
 124 solutions are partly performed by SBX. In [57], Tang and Wang proposed a novel hybrid multiobjective evolutionary algo-
 125 rithm (HMOEA). This approach uses multiple crossover operators to renew the evolved population. A self-adaptive selection
 126 mechanism is developed to determine an appropriate crossover operator from several candidates, i.e., BLX- α [22], SBX [10],
 127 SPX [59], PCX [11], and DE [56].

128 2.2. Motivation

129 The effect of crossover operator can be considered from two aspects: the chromosome level and the gene level [16]. The
 130 influence of chromosome level for crossover operator can be graphically investigated from Fig. 2 (a), where \$x^1 = \{x_1^1, x_2^1\}\$ and
 131 \$x^2 = \{x_1^2, x_2^2\}\$ denote two parent solutions with two genes, \$H_{x^1 x^2}\$ denotes the hyper cube enclosed by their genes. Regarding
 132 the effect of gene level, it can be graphically represented using a segment, as illustrated by \$S_{x_i^1 x_i^2}\$ in Fig. 2 (b).

133 Considering parent-centric crossover, the child solutions are usually attracted in the surroundings of the hyper cube's
 134 vertexes from chromosome level. This is because every gene is generated near to the parent gene in gene level, which
 135 makes the parent-centric crossover more suitable for the exploitation search. In mean-centric crossover, the child solutions
 136 are usually sampled around the center of \$H_{x^1 x^2}\$ from chromosome level, this is because every gene is generated near to
 137 the mean center of segment \$S_{x_i^1 x_i^2}\$ in gene level. In this sense, these two kinds of crossover operators are better for the
 138 exploitation search [16]. Although the existing hybrid approaches, such as HMOEA [57] and IMADE [45], attempting to solve
 139 the above problem by utilizing different crossover methods, it is still not an essential solution as the same crossover strategy
 140 is employed to produce every gene of a solution.

141 Working on the different direction, our proposed approach is combined by two state-of-the-art crossover operators, i.e.,
 142 SBX and DE, to produce each gene of a chromosome. The strong global search ability of DE is anticipated to well compensate
 143 the lack of exploration search in SBX. The intermediate results produced by SBX and DE can be easily exchanged by using

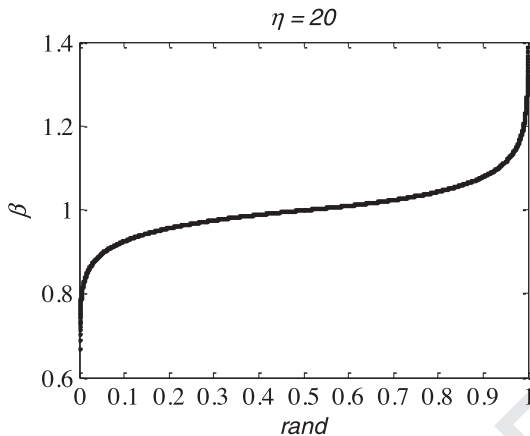


Fig. 3. The value range of β .

Algorithm 1

SBX operator for the i th gene bit.

Input: x_i^1, x_i^2
Output: c_i^1, c_i^2

- 1 use Eq. (2) to generate β
- 2 use Eq. (1) to generate c_i^1, c_i^2
- 3 return c_i^1, c_i^2

144 our proposed adaptive control approach. Therefore, it is reasonable and natural to combine the SBX and DE operators to
145 produce a new recombination operator.

146 **3. The proposed hybrid crossover operator**

147 In this section, our proposed AHX operator is introduced in detail. As AHX combines the merits of SBX and DE crossover
148 operators in gene level, brief introductions of SBX and DE are respectively given in Sections 3.1 and 3.2. After that, Section
149 3.3 shows the pseudo-code of AHX, which explains how to incorporate the merits of SBX and DE in gene level.

150 **3.1. SBX crossover operator**

151 Simulated binary crossover (SBX) was designed by Deb and Agrawal [10], which is applied to simulate the search pat-
152 tern of one-point binary crossover operator in real-coded representation. It is an important recombination operator used
153 in various multiobjective optimization algorithms [3,13,45,65,69]. Assume that $x^1 = \{x_1^1, \dots, x_n^1\}$ and $x^2 = \{x_1^2, \dots, x_n^2\}$ (n is the
154 dimension of decision variables) are two parents. After that, the variables c_i^1 and c_i^2 ($i=1,2,\dots,n$) in two children solution
155 $c^1 = \{c_1^1, \dots, c_n^1\}$ and $c^2 = \{c_1^2, \dots, c_n^2\}$ are computed as follows.

$$\begin{cases} c_i^1 = 0.5 \times [(1 + \beta) \cdot x_i^1 + (1 - \beta) \cdot x_i^2] \\ c_i^2 = 0.5 \times [(1 - \beta) \cdot x_i^1 + (1 + \beta) \cdot x_i^2] \end{cases} \quad (1)$$

156 where β follows the polynomial probability distribution and is calculated as follows.

$$\beta = \begin{cases} (2 \times \text{rand})^{1/(1+\eta)}, & \text{if } \text{rand} \leq 0.5 \\ \left(\frac{1}{2 - 2 \times \text{rand}}\right)^{1/(1+\eta)}, & \text{otherwise} \end{cases} \quad (2)$$

157 where the distribution index η is a predefined non-negative real number. A larger value of η will have more probabilities to
158 sample child solutions near to parent solutions. Generally, the value of η in SBX is commonly set to 15 or 20 [3,13,45,65,69].
159 Fig. 3 shows the potential values of β according to the random number rand when $\eta = 20$. As observed from Fig. 3, most
160 of the β values are located in [0.8, 1.2], which indicate that SBX has a large probability to get a β value near to 1.0. Based
161 on Eq. (1), a β value close to 1.0 will get c_i^1 and c_i^2 near to x_i^1 and x_i^2 . This means that SBX has strong local search ability
162 around the parent solutions. The pseudo-code of SBX for single gene bit is presented in Algorithm 1.

163 **3.2. DE crossover operator**

164 Differential evolution (DE) is a simple and directly search algorithm originally introduced by Storn and Price [56].
165 Many variants of DE were reported afterward, such as DE/rand/1/bin, DE/best/1/bin, DE/current-to-best/1/bin, DE/rand/2/bin,

Algorithm 2

HBX.

```

Input:  $x^1, x^2, x^3$  // three parent solutions
Output:  $y$  // the generated offspring solution
1   Set  $P_1$  and  $P_2$ 
2   if ( $rand < p_c$ )
3     for  $i = 1$  to  $n$ 
4       if ( $rand < P_1$ )
5         generate  $c_i^1, c_i^2$  from  $x_i^1, x_i^2$  use Algorithm 1
6         generate  $v_i$  from  $x_i^1, x_i^2, x_i^3$  by Eq. (3) with  $F=0.5$ 
7         if ( $rand < P_2$ )
8           if ( $rand < 0.5$ )
9              $y_i = c_i^2$ 
10            else
11               $y_i = c_i^1$ 
12            end if
13          else
14             $y_i = v_i$ 
15          end if
16        else
17           $y_i = x_i^2$ 
18        end if
19      end for
20    else
21       $y = x^1$ 
22    end if

```

166 DE/best/2/bin, which are mostly employed to solve single-objective optimization problems [46]. For example, the mutation
 167 operator of DE/rand/1/bin is given as follows

$$v_i = x_i^1 + F \times (x_i^2 - x_i^3) \quad (3)$$

168 where x^1 , x^2 and x^3 are the three distinct individuals selected from the evolved population, i denotes the i th gene for the
 169 selected individual, and F is a scaling factor controlling the mutant steps.

170 After mutation, a binomial crossover operation is applied to create the trial vector u as follows:

$$u_i = \begin{cases} v_i & \text{if } r_i \leq CR \text{ or } i = i_{rand} \\ x_i & \text{otherwise} \end{cases} \quad (4)$$

171 where i_{rand} is an integer randomly selected from $[1, n]$ (n is the dimension of decision variables) that guarantees at least one
 172 gene is inherited from the parent individual, r_i is a uniformly distributed random number in $[0, 1]$, and CR is the crossover
 173 probability usually ranged in $[0, 1]$.

174 DE/rand/1/bin has many important features, such as simple structure, ease of use, fast speed and robustness, which
 175 makes it very popular for global optimization [9]. The difference value between two genes $(x_i^2 - x_i^3)$ in **Eq. (3)** can be adap-
 176 tively adjusted according to the convergence situation of the evolved population. That is to say, DE/rand/1/bin uses a bigger
 177 mutation step to explore the entire decision space in the early stage, and a smaller mutation step for exploitation in the
 178 later stage.

179 **3.3. The proposed AHX operator**

180 **3.3.1. The hybrid crossover operator**

181 Based on the analysis in **Sections 3.1** and **3.2**, it can be concluded that SBX performs local search well with $\eta = 20$, while
 182 DE/rand/1 has a very powerful global search ability. Therefore, their advantages can be combined to provide the enhanced
 183 search capability, as investigated in [45,57]. However, the current studies [45,57] only consider the combination of SBX and
 184 DE in chromosome level, and thus the child individual is produced only using one specific crossover operator. In this pa-
 185 per, a novel hybrid crossover operator (HBX) is designed by combining SBX and DE in gene level. The local search ability
 186 of SBX and the global search ability of DE are jointly operated in the genes of a chromosome. This approach is aimed at
 187 providing better population diversity while maintaining a fast convergence speed. The pseudo-code of HBX is illustrated in
 188 **Algorithm 2**, where p_c is a crossover probability and $rand$ is a uniformly random number generated from $[0, 1]$. HBX pro-
 189 duces one child solution y from three parent solutions x^1, x^2, x^3 . For the generation of gene y_i , HBX obtains three genes
 190 c_i^1, c_i^2 and v_i by using the SBX and DE operations in three parent genes x_i^1, x_i^2, x_i^3 (lines 5 and 6), and then chooses the SBX
 191 results c_i^1, c_i^2 or the DE result v_i according to the probability P_2 (lines 7–15). Moreover, the use of the parameter P_1 is to
 192 control whether the gene is varied or not, which acts as a similar role as the CR parameter in **Eq. (4)**.

193 To graphically show the advantage of our proposed HBX operator, the distributions of solutions generated by SBX,
 194 DE/rand/1/bin and HBX are compared in **Fig. 4**. The two parent solutions are fixedly set as x^1 (0.3, 0.7) and x^2 (0.7, 0.3)
 195 for SBX, DE/rand/1/bin and HBX. Except that, every dimension of x^3 is randomly generated for DE/rand/1/bin and HBX.

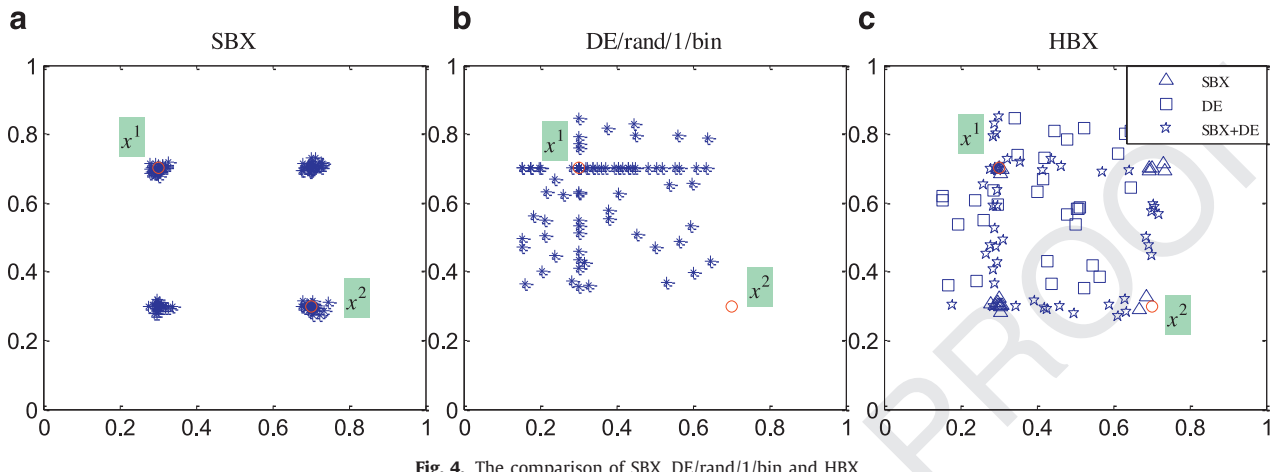


Fig. 4. The comparison of SBX, DE/rand/1/bin and HBX.

196 Fig. 4(a), (b)–(c) show 100 solutions produced by SBX, DE/rand/1/bin and HBX, respectively. From Fig. 4(a), it is observed
 197 that all genes of the child chromosomes are very near to the corresponding genes of the parents, while the child solutions
 198 obtained by DE seem more distributed around the first parent x^1 in Fig. 4(b). Thus, it is validated that DE has stronger
 199 global search ability than SBX. Especially, in Fig. 4 (c), the solutions marked with triangle are generated by SBX (lines 8–12
 200 in Algorithm 2) for every gene, while the solutions identified with square are obtained by DE (line 14 in Algorithm 2) for
 201 every gene. Except that, the solutions combining the genes produced by both SBX (lines 8–12 in Algorithm 2) and DE (line
 202 14 in Algorithm 2) are represented by the five-point star. These plots in Fig. 4 show that our HBX operator not only inherits
 203 the search patterns of SBX and DE, but also derives a new search pattern to combine SBX and DE on gene level (illustrated
 204 by the five-point star in Fig. 4 (c)), when compared to a simple combination of SBX and DE.

205 3.3.2. The adaptive parameter control approach

206 As introduced in Algorithm 2, P_1 and P_2 are two control parameters of HBX, in which P_1 decides the probability to
 207 perform crossover for certain gene and P_2 determines the probability to perform SBX or DE. It is noted that when P_1 is
 208 set to 1.0, the information from the parents are not inherited at all, and thus it will improve the population diversity.
 209 However, when P_1 is set to 0, all the children's genes are equal to x^2 , leading to no variation in population evolution. On
 210 the other hand, when the value of P_2 is larger, it has more chances to perform SBX for local search while a smaller value
 211 of P_2 owns more probabilities to execute DE for global search. To analyze the parameter sensitivity of P_1 and P_2 in HBX,
 212 HBX is embedded into a classical MOEA (NSGA-II). P_1 and P_2 are selected from {0.3, 0.9} and {0.1, 0.9} respectively. Due to
 213 space limitation, some representative results on ZDT1, WFG1, DTLZ1 and UF1 problems are shown in Fig. 5 with 4 different
 214 combinations of P_1 and P_2 . It can be observed that different combinations of P_1 and P_2 will greatly affect the optimization
 215 performance. The combinations of ($P_1 = 0.9$, $P_2 = 0.1$) and ($P_1 = 0.3$, $P_2 = 0.1$) have better population diversity, while the
 216 combinations of ($P_1 = 0.3$, $P_2 = 0.9$) and ($P_1 = 0.9$, $P_2 = 0.9$) have a faster convergence speed. Thus, the settings of P_1 and
 217 P_2 are sensitive to the performance of HBX operator, and thus an adaptive parameter control approach is further designed
 218 in this paper to balance the exploitation and exploration capabilities of HBX when solving various kinds of optimization
 219 problems.

220 It is experimentally found that global search capability is needed to search the entire space in the early stage of evo-
 221 lutionary process and local search capability is required to locate the better solutions around in the later stage [40,60].
 222 Therefore, P_1 is set to a large value in the early stage to perform hybrid crossover while P_2 is set to a small value to execute
 223 DE crossover for global search. At the later stage, another combination of P_1 and P_2 is demanded, where a small value of P_1
 224 is to keep the good genes that are historically explored and a large value of P_2 is assigned to operate SBX crossover for local
 225 search. Motivated by these considerations, an adaptive HBX (AHX) is designed for the above purposes. In AHX operator, P_1
 226 and P_2 are dynamically changed with evolutionary progress, which are formulated as follows.

$$P_1 = 0.7 \times \frac{1.0}{1 + \exp(20 \times (\frac{\text{evaluation}}{\text{max_evaluation}} - 0.25))} + 0.3 \quad (5)$$

$$P_2 = 0.8 \times \frac{1.0}{1 + \exp(-20 \times (\frac{\text{evaluation}}{\text{max_evaluation}} - 0.5))} + 0.1 \quad (6)$$

227 228 where *evaluation* and *max_evaluation* are respectively the current and maximum function evaluations. To graphically show
 229 the dynamic change of P_1 and P_2 , their tendencies are illustrated in Fig. 6, which shows that P_1 is reduced from 1.0 to 0.3,
 230 while P_2 is increased from 0.1 to 0.9 using a non-linear manner. These setting of P_1 (ranging from [0.3, 1.0]) and P_2 (ranging
 231 from [0.1, 0.9]) are obtained by running many experiments.

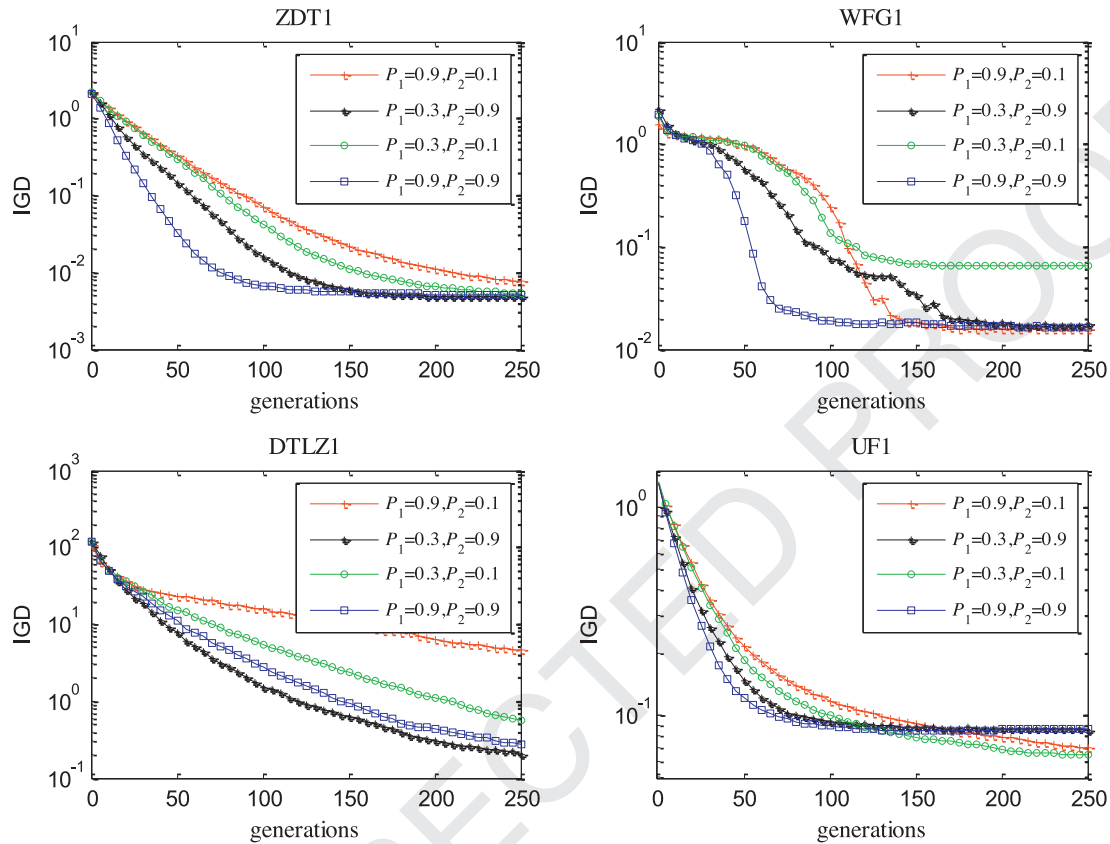


Fig. 5. The variation of the performance with different parameter settings.

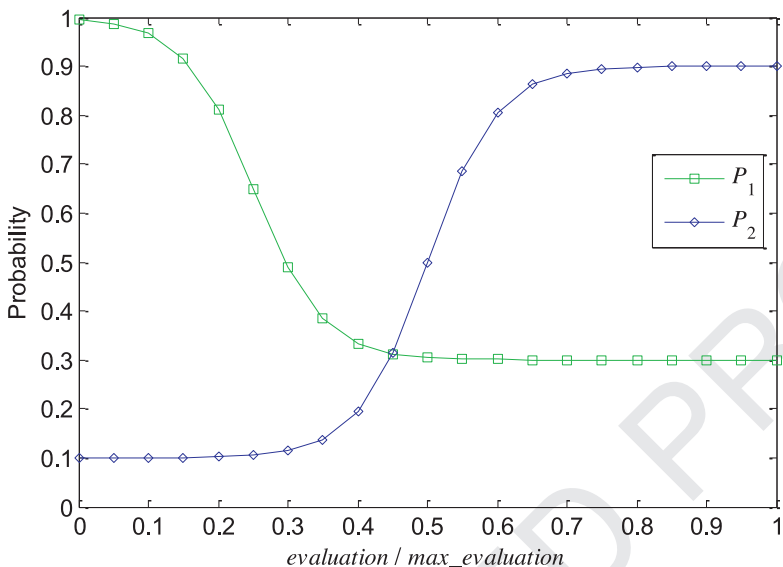
232 4. The experimental results

233 In order to validate the performance of our proposed operator, AHX is embedded into four state-of-the-art MOEAs, i.e.,
 234 NSGA-II [13], SPEA2 [69], SMS-EMOA [3], MOEA/D [65]. NSGA-II and SPEA2 are two of the most famous Pareto-based MOEAs,
 235 in which NSGA-II designs a fast non-dominated sorting approach and the crowding distance metric, while SPEA2 presents
 236 a novel fitness assignment strategy and k -nearest neighbor density estimation to maintain the population diversity. SMS-
 237 EMOA is an indicator-based MOEA, which maximizes the hyper-volume contribution value during the evolutionary process.
 238 Combined with the concept of non-dominated sorting, SMS-EMOA can get a solution set with very good convergence and
 239 diversity. MOEA/D [65] is a decomposition-based MOEA, in which MOPs are transformed into a set of single-objective op-
 240 timization problems and then each individual is assigned accordingly to optimize the corresponding subproblem. A modi-
 241 fied version of MOEA/D based on DE variance is presented in [40], named MOEA/D-DE. Both SBX-based MOEA/D [65] and
 242 DE-based MOEA/D [40] are included for comparison. Moreover, to further validate the effectiveness of AHX, it is further
 243 compared to three recently proposed hybrid crossover operators, i.e., DEI [45], JGBL [37] and FRRMAB [34]. In the following
 244 subsections, the test problems and performance metrics used in this study are described in Sections 4.1 and 4.2, respectively.
 245 Then, the parameter settings for all the compared algorithms are described in Section 4.3. At last, the comparative results
 246 are given in Sections 4.4 and 4.5.

247 4.1. Test problems

248 A number of well-known test problems are adopted here to validate the effectiveness of our proposed AHX operator.
 249 These test functions are commonly used in the literature [4,13,40,45,65,69] and they can be divided into two categories
 250 according to the number of objectives.

251 Considering the bi-objective test problems, the most widely used ZDT suite [67] (ZDT1-ZDT4, and ZDT6) is selected. Due
 252 to the lack of some features in ZDT test suite, such as variable linkage and multi-modality, it is not too hard to solve the
 253 ZDT test suite. Therefore, the walking fish group (WFG) test suite (WFG1-WFG9) [25] is included, which is characterized
 254 with various features, such as non-separable, deceptive, degenerate problems, mixed PF shape, variable dependencies, and
 255 multi-modality. Moreover, the complicated PS test suite (UF1-UF7) [64] is also used for comparison. Regarding to the

Fig. 6. The tendency for P_1 and P_2 .

256 three-objective test problems, the DTLZ test suite [14] and UF8-UF10 [64] are utilized. The numbers of decision variables
 257 are set to 30 for ZDT1-ZDT3 and UF1-UF10, and 10 for ZDT4, ZDT6 and all of WFG and DTLZ test problems. Especially for
 258 WFG test problems, 10 decision variables are composed by 8 position parameters and 2 distance parameters. Totally, 31
 259 test functions (i.e., ZDT1-ZDT4, ZDT6, WFG1-WFG9, DTLZ1-DTLZ7, and UF1-UF10) are covered in our experimental studies,
 260 which make the comparison results more comprehensive and convincing.

261 4.2. Performance metrics

262 As discussed in [26] and [71], no unary performance metric is able to give a comprehensive measure on the performance
 263 of an MOEA. In order to assess the performance among the compared algorithms, two performance metrics, i.e. the inverted
 264 generational distance (IGD) [40] and hyper-volume (HV) [70] are adopted. They are commonly used in many MOEAs for
 265 performance evaluation [3,13,40,45,65,69].

266 (1) IGD metric

267 IGD metric measures the mean distance from each point of the true Pareto set to the nearest solution of the approximate
 268 set in the objective space. This inverted generational distance can provide reliable information on both the diversity
 269 and convergence of obtained solutions. Mathematically, let P^* denote a subset of Pareto-optimal solutions uniformly
 270 distributed along the true PF and P represent the approximate set obtained by MOEAs. Then, the IGD value from P^*
 271 to P is calculated as follows.

$$272 \text{IGD} = \sum_{z \in P^*} \frac{d(z, P)}{|P^*|} \quad (7)$$

273 where, $|P^*|$ denotes the size of P^* (i.e. the number of solutions in P^*), $d(z, P)$ returns the minimal Euclidean distance
 274 from point z to P . A smaller IGD value denotes that the approximate set is closer to the true PF and distributed more
 275 uniformly. It is noted that the true PF has to be available in advance when calculating the IGD metric. In our experiments,
 276 the true PF of each test problem can be publicly downloaded from <http://jmetal.sourceforge.net/problems.html>,
 and the number of $|P^*|$ for each test problem is shown in Table 1.

277 (2) HV metric

278 HV metric calculates the size of the objective space that is dominated by the approximate set S and bounded by a
 279 reference point $z^r = (z_1^r, \dots, z_m^r)^T$ that is dominated by all points on the true PF. The calculation of HV metric is given
 280 as follows:

$$281 \text{HV}(S) = \text{Vol}(\bigcup_{x \in S} [f_1(x), z_1^r] \times \dots \times [f_m(x), z_m^r]) \quad (8)$$

282 where, $\text{Vol}(\cdot)$ denotes the Lebesgue measure. It is important to note that, when calculating the HV value, the points that
 283 cannot dominate the reference point will be discarded (i.e. a solution that has an objective worse than the reference
 point does not have any contribution to HV).

Table 1
Number of Points for the True PF.

Problem	Points	Problem	Points	Problem	Points	Problem	Points
ZDT1	1001	DTLZ4	4000	WFG5	2601	UF4	1000
ZDT2	1001	DTLZ5	333	WFG6	2601	UF5	21
ZDT3	269	DTLZ6	140	WFG7	2601	UF6	1000
ZDT4	1001	DTLZ7	676	WFG8	10201	UF7	1000
ZDT6	1001	WFG1	605	WFG9	2601	UF8	10000
DTLZ1	10000	WFG2	111	UF1	1000	UF9	10000
DTLZ2	10000	WFG3	301	UF2	1000	UF10	10000
DTLZ3	4000	WFG4	1181	UF3	1000	–	–

Table 2
Setting of reference points.

Test instance	Reference point
ZDT1-ZDT4, ZDT6, UF1-UF7	(2.0, 2.0)
DTLZ1	(1.0, 1.0, 1.0)
DTLZ2-DTLZ6, UF8-UF10	(2.0, 2.0, 2.0)
DTLZ7	(2.0, 2.0, 7.0)
WFG1-WFG9	(3.0, 5.0)

Table 3

IGD Comparison (Median and IQR) of NSGA-II with different variance.

Problems	NSGA-II-SBX \tilde{x}_{IQR}	NSGA-II-DE \tilde{x}_{IQR}	NSGA-II-HBX \tilde{x}_{IQR}	NSGA-II-AHX \tilde{x}_{IQR}
ZDT1	4.931e-03 3.04e-04 –	7.717e-02 2.48e-02 –	4.858e-03 3.07e-04 ≈	4.795e-03 2.03e-04
ZDT2	5.015e-03 2.38e-04 –	2.358e-01 1.64e-01 –	4.797e-03 2.25e-04 ≈	4.860e-03 2.20e-04
ZDT3	5.357e-03 2.89e-04 –	9.186e-02 7.15e-02 –	5.206e-03 1.51e-04 ≈	5.233e-03 2.34e-04
ZDT4	6.252e-03 1.43e-03 ≈	2.356e+01 4.51e+00 –	4.687e-03 2.36e-04 +	5.999e-03 4.04e-03
ZDT6	8.756e-03 1.22e-03 –	4.060e-03 1.16e-03 ≈	3.982e-03 6.45e-04 +	4.344e-03 6.97e-04
WFG1	1.580e+00 1.85e-01 –	1.654e-02 1.60e-02 ≈	1.552e-02 1.35e-03 ≈	1.547e-02 1.37e-03
WFG2	7.253e-02 1.67e-01 –	1.156e-02 1.52e-03 +	6.660e-02 1.12e-03 –	6.595e-02 5.42e-02
WFG3	3.907e-01 6.19e-03 –	3.856e-01 5.59e-04 ≈	3.852e-01 5.59e-04 ≈	3.853e-01 7.05e-04
WFG4	1.383e-02 1.53e-03 ≈	1.378e-02 1.02e-03 ≈	1.353e-02 1.52e-03 ≈	1.351e-02 1.22e-03
WFG5	6.780e-02 3.22e-04 ≈	6.872e-02 8.95e-04 –	6.784e-02 6.14e-04 ≈	6.772e-02 6.29e-04
WFG6	1.648e-02 1.73e-03 ≈	1.651e-02 1.02e-03 –	1.643e-02 1.13e-03 ≈	1.602e-02 8.93e-04
WFG7	1.725e-02 3.22e-03 –	1.601e-02 9.73e-04 ≈	1.598e-02 1.51e-03 ≈	1.614e-02 1.19e-03
WFG8	3.980e-02 7.44e-03 –	2.305e-02 1.53e-03 +	3.981e-02 6.70e-03 –	3.466e-02 7.27e-03
WFG9	1.550e-02 8.95e-04 ≈	1.911e-02 1.52e-03 –	1.577e-02 1.01e-03 ≈	1.552e-02 4.88e-04
DTLZ1	6.702e-01 6.11e-01 –	5.743e+00 7.71e+00 –	2.827e-02 6.41e-03 ≈	2.726e-02 7.20e-03
DTLZ2	6.961e-02 3.75e-03 ≈	7.238e-02 3.97e-03 –	6.641e-02 2.86e-03 ≈	6.718e-02 3.55e-03
DTLZ3	2.162e+00 1.64e+00 –	1.893e+01 1.63e+01 –	7.007e-02 8.55e-03 +	7.663e-02 1.45e-02
DTLZ4	6.201e-02 9.82e-03 ≈	7.518e-02 6.69e-03 –	6.395e-02 7.08e-03 –	6.121e-02 7.89e-03
DTLZ5	5.563e-03 3.27e-04 ≈	6.765e-03 6.88e-04 –	5.621e-03 2.64e-04 ≈	5.624e-03 3.63e-04
DTLZ6	5.433e-01 7.09e-02 –	4.921e-03 2.50e-04 +	5.737e-03 2.21e-04 +	6.057e-03 3.50e-04
DTLZ7	7.642e-02 5.92e-03 ≈	8.703e-02 8.56e-03 –	7.448e-02 4.55e-03 ≈	7.406e-02 4.66e-03
UF1	1.011e-01 5.09e-02 –	1.079e-01 3.53e-02 –	8.205e-02 8.37e-03 ≈	8.220e-02 1.16e-02
UF2	4.144e-02 6.23e-03 –	6.584e-02 1.02e-02 –	4.017e-02 8.15e-03 ≈	3.926e-02 6.24e-03
UF3	2.109e-01 4.61e-02 +	2.141e-01 2.24e-02 +	3.778e-01 3.11e-02 –	2.618e-01 2.44e-02
UF4	5.878e-02 2.52e-03 –	7.764e-02 1.23e-02 –	4.828e-02 2.43e-03 –	4.702e-02 1.57e-03
UF5	5.261e-01 2.06e-01 –	1.761e+00 4.79e-01 –	3.753e-01 1.54e-01 ≈	3.153e-01 2.06e-01
UF6	2.831e-01 1.24e-01 ≈	7.235e-01 1.85e-01 –	3.276e-01 9.63e-02 –	2.204e-01 1.38e-01
UF7	8.158e-02 2.27e-01 –	9.479e-02 4.47e-02 –	4.050e-02 7.59e-03 +	4.204e-02 4.58e-03
UF8	2.232e-01 2.48e-02 +	7.258e-01 4.49e-01 –	3.571e-01 9.47e-02 –	2.664e-01 7.34e-02
UF9	3.363e-01 1.14e-01 +	8.218e-01 4.07e-01 –	5.860e-01 1.92e-01 –	5.193e-01 1.48e-01
UF10	6.947e-01 4.62e-01 +	3.976e+00 6.36e-01 –	2.097e+00 8.33e-01 –	1.178e+00 1.02e+00
-/+≈	17/4/10	22/4/5	9/5/17	-/-

The symbols of “–”, “+” and “≈” denote the corresponding value is significantly worse than, better than, and similar to that of NSGA-II-AHX according to the Wilcoxon's rank sum test with the 5% significance level, respectively.

Table 4

HV Comparison (Median and IQR) of NSGA-II with different variance.

Problems	NSGA-II-SBX \tilde{x} IQR	NSGA-II-DE \tilde{x} IQR	NSGA-II-HBX \tilde{x} IQR	NSGA-II-AHX \tilde{x} IQR
ZDT1	3.6589 6.06e-04 –	3.4888 6.42e-02 –	3.6599 3.48e-04 –	3.6602 2.97e-04
ZDT2	3.3245 7.57e-04 –	2.5169 5.69e-01 –	3.3269 4.10e-04 –	3.3271 3.60e-04
ZDT3	4.8127 5.07e-04 –	4.3099 2.69e-01 –	4.8142 3.18e-04 –	4.8145 2.24e-04
ZDT4	3.6514 6.43e-03 ≈	0.0000 0.00e+00 –	3.6599 5.68e-04 +	3.6548 1.30e-02
ZDT6	3.0208 3.11e-03 –	3.0411 3.07e-04 +	3.0400 3.69e-04 +	3.0395 4.29e-04
WFG1	6.4476 2.26e+00 –	12.056 5.69e-02 –	12.062 2.95e-03 ≈	12.062 4.47e-03
WFG2	10.578 1.33e+00 –	11.456 1.65e-03 ≈	10.623 9.75e-04 –	10.624 8.33e-01
WFG3	10.909 1.80e-02 –	10.928 4.09e-03 –	10.939 6.30e-03 ≈	10.939 5.13e-03
WFG4	8.5238 6.06e-02 –	8.4615 4.38e-02 –	8.5905 3.25e-02 –	8.6188 2.86e-02
WFG5	8.0793 1.91e-02 ≈	7.8259 7.58e-02 –	8.0480 4.72e-02 –	8.0837 3.59e-02
WFG6	8.4347 1.87e-01 –	8.6647 3.95e-03 –	8.6686 2.58e-01 –	8.6735 3.49e-03
WFG7	7.6543 3.71e-01 –	8.6658 5.53e-03 ≈	8.3021 4.96e-03 –	8.3191 3.61e-01
WFG8	7.9509 2.00e-01 –	8.0752 1.66e-01 –	8.2007 7.42e-02 –	8.2826 9.60e-02
WFG9	8.3364 3.49e-02 –	8.1656 7.05e-02 –	8.3330 4.14e-02 –	8.3509 3.35e-02
DTLZ1	0.2107 3.97e-01 –	0.0000 0.00e+00 –	0.9681 2.68e-03 ≈	0.9684 4.19e-03
DTLZ2	7.3580 1.68e-02 –	7.3469 5.87e-03 –	7.3759 6.54e-03 ≈	7.3778 5.43e-03
DTLZ3	0.0000 3.83e-01 –	0.0000 0.00e+00 –	7.3627 2.21e-02 ≈	7.3455 6.08e-02
DTLZ4	7.3722 2.44e-02 –	7.3437 1.12e-02 –	7.3756 5.68e-03 –	7.3845 6.73e-03
DTLZ5	6.0989 8.03e-04 ≈	6.0917 1.20e-03 –	6.0978 8.98e-04 –	6.0987 7.87e-04
DTLZ6	4.5293 2.76e-01 –	6.1017 5.77e-04 +	6.0999 8.68e-04 +	6.0992 1.08e-03
DTLZ7	13.308 6.25e-02 ≈	12.987 2.08e-01 –	13.329 6.90e-02 ≈	13.317 7.06e-02
UF1	3.3321 1.14e-01 –	3.4286 1.03e-01 –	3.4808 1.64e-01 –	3.5246 1.80e-02
UF2	3.5325 6.36e-02 –	3.5247 2.94e-02 –	3.5726 5.75e-02 –	3.6010 1.17e-02
UF3	2.7310 9.11e-02 –	3.3328 3.65e-02 +	2.8187 1.10e-01 –	3.2439 1.39e-01
UF4	3.1752 1.03e-02 –	3.1185 5.08e-02 –	3.2042 7.10e-03 ≈	3.2053 4.80e-03
UF5	1.8072 3.73e-01 –	0.0497 1.76e-01 –	2.2268 6.96e-01 –	2.7988 8.06e-01
UF6	2.5387 4.05e-01 –	1.5178 3.52e-01 –	2.4809 2.65e-01 ≈	2.9058 5.66e-01
UF7	3.3050 7.31e-01 –	3.2896 7.54e-02 –	3.4271 4.09e-02 ≈	3.4253 2.34e-02
UF8	6.3316 1.50e-01 +	3.0141 2.32e+00 –	5.7498 5.06e-01 –	6.1658 2.54e-01
UF9	5.9677 6.10e-01 ≈	2.9262 1.99e+00 –	5.0264 1.30e+00 –	5.6746 1.35e+00
UF10	2.8354 1.51e+00 +	0.0000 0.00e+00 –	0.0081 1.95e-01 –	1.1955 4.05e+00
–/+/≈	24/2/5	26/3/2	19/3/9	–/-/-

The symbols of “–”, “+” and “≈” denote the corresponding value is significantly worse than, better than, and similar to that of NSGA-II-AHX according to the Wilcoxon's rank sum test with the 5% significance level, respectively.

284 For each objective, an integer larger than the worst value of the corresponding objective in the true PF is adopted as the
285 reference point, which is similar to [38,34,31]. In our experiments, the reference points for all the test instances are
286 illustrated in Table 2.

287 4.3. The parameter settings

288 To have a fair comparison, the SBX and polynomial mutation operators in all compared algorithms have the same pa-
289 rameter settings. The crossover probability and distribution index of SBX are respectively set to 0.9 and 20. The mutation
290 probability of polynomial mutation is set to $1/n$, where n is the number of decision variables for each test problem. The
291 distribution index for polynomial mutation is set to 20. The CR and F value in DE operator are respectively set to 1.0 and
292 0.5 as suggested in [38,34,40].

293 Tournament selection approach is adopted in NSGA-II, SPEA2, and SMS-EMOA to select the evolved population. The mat-
294 tching parents of MOEA/D and IMADE are picked out from the neighboring solutions with a probability of 0.9 or from the
295 entire population otherwise.

296 Each algorithm is implemented by Java programming language in the framework of jMetal, which facilitates the de-
297velopment of metaheuristics for tackling MOPs [19]. The population size in each algorithm is set to 100. Each algorithm is
298 executed 30 runs independently for each test instance on a computer with a configuration of Intel Core i7-4770 CPU 3.4 GHz
299 processor and 8.0GB memory. The maximum number of function evaluations is set to 25,000 for all the test instances.

Table 5

IGD Comparison (Median and IQR) of SPEA2 with different variance.

Problems	SPEA2-SBX \tilde{x} IQR	SPEA2-DE \tilde{x} IQR	SPEA2-HBX \tilde{x} IQR	SPEA2-AHX \tilde{x} IQR
ZDT1	4.182e-03 1.20e-04 -	2.867e-01 6.97e-02 -	3.932e-03 5.08e-05 -	3.901e-03 7.81e-05
ZDT2	4.304e-03 2.31e-04 -	4.930e-01 1.82e-01 -	3.934e-03 4.11e-05 -	3.903e-03 6.36e-05
ZDT3	5.060e-03 2.20e-04 -	3.378e-01 1.05e-01 -	4.829e-03 1.82e-04 ≈	4.766e-03 1.78e-04
ZDT4	6.575e-03 8.15e-03 ≈	2.484e+01 4.43e+00 -	4.027e-03 2.01e-04 +	9.674e-03 9.77e-03
ZDT6	1.458e-02 2.11e-03 -	2.660e-03 2.75e-04 ≈	2.766e-03 1.49e-04 ≈	2.684e-03 1.85e-04
WFG1	1.749e+00 5.06e-02 -	1.173e-01 3.21e-01 -	1.277e-02 5.35e-04 ≈	1.260e-02 3.40e-04
WFG2	7.126e-02 1.68e-01 -	1.040e-02 1.48e-03 +	6.534e-02 8.03e-04 -	6.474e-02 5.46e-02
WFG3	4.157e-01 1.89e-02 -	3.837e-01 2.75e-04 -	3.833e-01 2.83e-04 -	3.832e-01 1.72e-04
WFG4	1.223e-02 5.87e-04 +	1.383e-02 1.50e-03 -	1.280e-02 7.05e-04 ≈	1.253e-02 7.14e-04
WFG5	6.665e-02 1.43e-04 -	6.836e-02 1.54e-03 -	6.652e-02 1.67e-04 ≈	6.648e-02 2.12e-04
WFG6	1.345e-02 1.80e-03 -	1.306e-02 4.82e-04 ≈	1.296e-02 8.80e-04 ≈	1.278e-02 5.90e-04
WFG7	1.912e-02 9.74e-03 -	1.330e-02 7.74e-04 -	1.309e-02 6.07e-04 ≈	1.296e-02 5.88e-04
WFG8	5.117e-02 9.54e-03 -	4.303e-02 9.67e-03 ≈	4.782e-02 9.44e-03 -	4.061e-02 6.55e-03
WFG9	1.285e-02 7.69e-04 ≈	1.698e-02 1.55e-03 -	1.281e-02 5.24e-04 ≈	1.276e-02 4.79e-04
DTLZ1	3.518e-01 5.26e-01 -	5.013e+00 8.24e+00 -	2.496e-02 4.02e-03 ≈	2.627e-02 1.51e-02
DTLZ2	5.452e-02 1.39e-03 ≈	6.683e-02 2.81e-03 -	5.610e-02 1.09e-03 -	5.428e-02 1.37e-03
DTLZ3	1.492e+00 1.14e+00 -	7.860e+00 1.59e+01 -	6.280e-02 1.71e-02 ≈	6.068e-02 1.70e-02
DTLZ4	4.750e-02 1.14e-01 -	6.540e-02 7.22e-03 -	4.663e-02 7.83e-03 -	4.217e-02 5.48e-03
DTLZ5	4.419e-03 1.61e-04 ≈	1.059e-02 1.04e-03 -	4.715e-03 1.69e-04 -	4.398e-03 1.85e-04
DTLZ6	4.642e-01 5.84e-02 -	4.152e-03 1.62e-04 -	4.037e-03 1.31e-04 ≈	4.055e-03 1.50e-04
DTLZ7	6.066e-02 2.05e-03 -	6.712e-02 4.38e-03 -	5.896e-02 1.50e-03 -	5.769e-02 1.44e-03
UF1	1.063e-01 1.72e-02 -	9.453e-02 2.77e-02 -	8.813e-02 1.62e-02 ≈	8.727e-02 2.03e-02
UF2	5.184e-02 3.82e-03 -	6.471e-02 6.95e-03 -	4.383e-02 7.46e-03 ≈	4.152e-02 5.23e-03
UF3	2.251e-01 4.22e-02 +	2.372e-01 4.11e-02 +	3.712e-01 2.48e-02 -	3.124e-01 5.09e-02
UF4	6.154e-02 3.63e-03 -	7.313e-02 1.28e-02 -	4.899e-02 2.49e-03 -	4.767e-02 2.54e-03
UF5	3.857e-01 1.69e-01 -	1.745e+00 5.02e-01 -	3.886e-01 2.79e-01 -	3.122e-01 6.30e-02
UF6	2.367e-01 6.76e-02 ≈	6.136e-01 1.69e-01 -	2.472e-01 2.18e-01 ≈	2.070e-01 1.37e-01
UF7	2.857e-01 2.93e-01 -	5.947e-02 2.94e-02 -	4.224e-02 7.83e-03 ≈	4.792e-02 1.13e-02
UF8	1.972e-01 1.24e-02 ≈	2.993e-01 1.11e-01 -	2.274e-01 1.52e-02 -	1.936e-01 1.39e-02
UF9	2.413e-01 7.05e-02 ≈	4.365e-01 2.09e-01 -	2.506e-01 8.16e-02 +	2.775e-01 6.46e-02
UF10	3.983e-01 1.79e-01 ≈	3.050e+00 3.99e-01 -	7.371e-01 1.45e-01 -	3.038e-01 1.77e-01
-/+≈	21/2/8	26/2/3	14/2/15	-/-

The symbols of “-”, “+” and “≈” denote the corresponding value is significantly worse than, better than, and similar to that of SPEA2-AHX according to the Wilcoxon's rank sum test with the 5% significance level, respectively.

300 4.4. Performance verification of AHX

301 Our proposed operator AHX is compared with SBX, DE and HBX (the parameters P_1 and P_2 in HBX are fixedly set to
302 0.5). All these crossover operators are embedded into the framework of NSGA-II, SPEA2, SMS-EMOA, and MOEA/D, and the
303 revised algorithms are named NSGA-II-(SBX, DE, HBX, AHX), SPEA2-(SBX, DE, HBX, AHX), SMS-EMOA-(SBX, DE, HBX, AHX),
304 and MOEA/D-(SBX, DE, HBX, AHX) respectively. Note that the original crossover operator in NSGA-II [13], SPEA2 [69], and
305 SMS-EMOA [3] is SBX, while MOEA/D has the SBX-based [65] and DE-based versions [40]. The experimental results are
306 collected in each table, which lists the median \bar{x} and the interquartile range IQR over 30 independent runs. The best one
307 for each problem is highlighted in dark grey background and the second best ones for each problem is marked in light
308 grey background. In addition, the Wilcoxon rank sum test is used to distinguish the statistic difference of the revised AHX-
309 based algorithms with the original algorithms on each test problem. The symbols “-”, “+” and “≈” respectively indicate that
310 the performance of the corresponding algorithm is worse than, better than, and similar to that of the revised AHX-based
311 algorithm according to the Wilcoxon rank sum test at a 5% significance level.

312 4.4.1. The comparison in the frameworks of different MOEAs

313 (1) The comparison of the four evolutionary operators in NSGA-II

314 At first, NSGA-II-AHX is compared with NSGA-II-SBX, NSGA-II-DE, and NSGA-II-HBX. The results of 31 test problems re-
315 garding to the IGD and HV metrics are given in Tables 3 and 4, respectively. For the IGD metric in Table 3, when compared to
316 NSGA-II-SBX, the performance of NSGA-II-AHX has a significant improvement when the SBX operator in NSGA-II is replaced
317 by AHX, as NSGA-II-AHX achieves the better, similar and worse results respectively in 17, 4 and 10 out of 31 test problems.
318 Especially, the performance improvement is noticeable for some cases, such as WFG1, WFG2, DTLZ1, DTLZ3, DTLZ6, UF1,

Table 6

HV Comparison (Median and IQR) of SPEA2 with different variance.

Problems	SPEA2-SBX \tilde{x} IQR	SPEA2-DE \tilde{x} IQR	SPEA2-HBX \tilde{x} IQR	SPEA2-AHX \tilde{x} IQR
ZDT1	3.6587 9.54e-04 –	2.9413 2.12e-01 –	3.6609 2.73e-04 –	3.6613 1.94e-04
ZDT2	3.3229 2.98e-03 –	1.8840 4.31e-01 –	3.3275 3.38e-04 –	3.3280 2.77e-04
ZDT3	4.8108 1.25e-03 –	3.3963 3.44e-01 –	4.8132 4.15e-04 –	4.8140 5.39e-04
ZDT4	3.6477 5.98e-02 ≈	0.0000 0.00e+00 –	3.6603 7.04e-04 +	3.6395 3.20e-02
ZDT6	3.0050 5.35e-03 –	3.0418 6.05e-05 –	3.0418 2.82e-05 ≈	3.0418 2.77e-05
WFG1	5.6019 2.25e+00 –	11.641 1.33e+00 –	12.067 4.12e-03 –	12.069 2.45e-03
WFG2	10.581 1.33e+00 –	11.457 5.92e-03 ≈	10.624 1.31e-03 –	10.625 8.34e-01
WFG3	10.810 9.32e-02 –	10.942 3.56e-03 –	10.950 3.82e-03 –	10.952 2.48e-03
WFG4	8.3636 1.32e-01 –	8.4457 4.12e-02 –	8.5152 6.23e-02 –	8.5679 4.02e-02
WFG5	7.9792 3.72e-02 –	7.7233 1.09e-01 –	7.9488 6.39e-02 –	8.0335 7.00e-02
WFG6	8.3270 1.65e-01 –	8.6740 2.28e-03 –	8.6730 1.61e-02 –	8.6789 4.61e-03
WFG7	7.2762 2.84e-01 –	8.6657 9.42e-01 ≈	8.2879 3.71e-02 –	8.3101 3.84e-01
WFG8	7.4696 2.89e-01 –	7.6137 1.82e-01 –	8.0233 6.87e-02 –	8.1214 1.04e-01
WFG9	8.2975 6.44e-02 –	8.1649 9.29e-02 –	8.3131 5.51e-02 ≈	8.3147 5.79e-02
DTLZ1	0.6836 5.74e-01 –	0.0000 0.00e+00 –	0.9709 2.16e-03 ≈	0.9701 6.58e-03
DTLZ2	7.3983 1.04e-02 –	7.3664 6.84e-03 –	7.4010 3.80e-03 –	7.4088 3.63e-03
DTLZ3	0.0000 1.48e+00 –	0.0000 6.26e-01 –	7.3729 3.74e-02 ≈	7.3770 3.32e-02
DTLZ4	7.3991 9.84e-01 –	7.3502 9.06e-03 –	7.3995 4.48e-03 –	7.4088 3.49e-03
DTLZ5	6.1013 6.60e-04 ≈	6.0814 3.51e-03 –	6.0996 9.61e-04 –	6.1015 6.51e-04
DTLZ6	4.7158 1.59e-01 –	6.1030 1.86e-04 –	6.1032 1.45e-04 ≈	6.1032 1.04e-04
DTLZ7	13.442 1.94e-02 –	13.078 1.28e-01 –	13.454 2.43e-02 –	13.477 1.78e-02
UF1	3.3271 9.69e-02 –	3.4698 1.03e-01 –	3.4644 1.67e-01 –	3.5186 2.80e-02
UF2	3.5019 7.37e-02 –	3.5264 3.53e-02 –	3.5451 5.37e-02 –	3.5916 1.13e-02
UF3	2.6218 8.60e-02 –	3.2890 5.74e-02 +	2.7892 5.58e-02 –	3.1811 3.38e-01
UF4	3.1657 1.16e-02 –	3.1206 3.38e-02 –	3.2007 5.81e-03 ≈	3.2033 5.69e-03
UF5	2.1270 4.33e-01 –	0.0648 1.63e-01 –	2.2190 6.37e-01 –	2.8629 5.13e-01
UF6	2.6349 2.96e-01 –	1.8089 3.42e-01 –	2.6332 6.54e-01 ≈	2.9652 5.01e-01
UF7	2.6165 8.12e-01 –	3.3575 7.39e-02 –	3.4104 6.24e-02 ≈	3.4193 6.01e-02
UF8	6.3310 3.27e-02 ≈	5.7869 5.94e-01 –	6.1842 6.67e-02 –	6.3374 6.38e-02
UF9	5.8251 4.39e-01 –	5.3614 1.45e+00 –	6.6270 5.49e-01 ≈	6.5881 8.82e-01
UF10	3.9762 2.21e+00 ≈	0.0000 0.00e+00 –	3.1966 8.28e-01 –	5.6584 1.29e+00
–/+≈	27/0/4	28/1/2	21/1/9	–/-

The symbols of “–”, “+” and “≈” denote the corresponding value is significantly worse than, better than, and similar to that of SPEA2-AHX according to the Wilcoxon's rank sum test with the 5% significance level, respectively.

and UF5. Regarding to the comparison of NSGA-II-AHX with NSGA-II-DE, NSGA-II-AHX performs better than, similarly with and worse than NSGA-II-DE in 22, 5 and 4 out of 31 test instances. NSGA-II-DE gets worse results in ZDT1-ZDT4, DTLZ1, DTLZ3, UF1, UF2, UF4-UF10. This is because the CR value is set to 1.0 in NSGA-II-DE, and resultantly no gene information is inherited from parent population. Clearly, NSGA-II-AHX performs significantly better than NSGA-II-SBX and NSGA-II-DE on the IGD metric. For the HV metric results in Table 4, similar comparison results are observed. NSGA-II-AHX is respectively better than NSGA-II-SBX and NSGA-II-DE on 24 and 26 out of 31 test problems. This validates the advantages of the proposed AHX operator when compared to the SBX and DE operators. AHX can have a better balance between the exploration and exploitation capabilities in the framework of NSGA-II when compared to SBX and DE.

In order to investigate the effectiveness of our proposed adaptive parameter control approach in AHX, NSGA-II-AHX is further compared with NSGA-II-HBX (the parameters P_1 and P_2 are fixedly set to 0.5 in NSGA-II-HBX). The IGD and HV comparison results are shown in the last two columns of Tables 3 and 4. It can be observed that NSGA-II-AHX is respectively better than, worse than, and similar to NSGA-II-HBX on 9, 5, and 17 out of 31 test problems for the IGD metric. For the HV metric, NSGA-II-AHX is respectively better than, worse than, and similar to NSGA-II-HBX on 19, 3, and 9 out of 31 test problems. It is interesting to point out that AHX is especially enhanced by the adaptive parameter control approach when tackling the WFG and UF test suites. It may be due to that the adaptive parameter control approach is especially effective to enhance the search capability for solving complicated problems. Therefore, it is reasonable to conclude that our proposed adaptive parameter control approach is able to enhance the performance of AHX.

It is worth noting that when compared with the other three operators (SBX, DE, and HBX) in NSGA-II, AHX always achieves the first or second ranks on all the test problems except ZDT6, WFG8, DTLZ6, DTLZ7, and UF3 on the IGD metric in Table 3. Considering the HV metric in Table 4, AHX also obtains the first or second ranks on all the test problems except

Table 7

IGD Comparison (Median and IQR) of SMS-EMOA with different variance.

Problems	SMS-EMOA-SBX \tilde{x}_{IQR}	SMS-EMOA-DE \tilde{x}_{IQR}	SMS-EMOA-HBX \tilde{x}_{IQR}	SMS-EMOA-AHX \tilde{x}_{IQR}
ZDT1	3.644e-03 3.25e-05 ≈	2.036e-01 5.71e-02 -	3.622e-03 2.39e-05 +	3.646e-03 3.41e-05
ZDT2	4.395e-03 1.79e-04 ≈	3.201e-01 2.06e-01 -	4.364e-03 1.34e-04 ≈	4.359e-03 1.54e-04
ZDT3	4.159e-03 3.50e-05 ≈	2.423e-01 1.50e-01 -	4.153e-03 5.17e-05 +	4.174e-03 6.88e-05
ZDT4	1.663e-02 1.82e-02 ≈	2.102e+01 8.64e+00 -	3.673e-03 4.80e-05 +	5.245e-03 1.41e-02
ZDT6	4.276e-03 6.72e-04 -	2.673e-03 2.14e-04 ≈	2.683e-03 1.77e-04 ≈	2.619e-03 1.27e-04
WFG1	1.885e+00 1.82e-01 -	3.202e-02 2.41e-02 -	1.487e-02 5.16e-04 ≈	1.485e-02 4.44e-04
WFG2	7.100e-02 1.68e-01 -	1.115e-02 5.42e-02 +	6.566e-02 6.91e-04 -	6.549e-02 5.09e-04
WFG3	4.337e-01 4.42e-02 -	3.827e-01 7.39e-06 +	3.827e-01 2.44e-05 -	3.827e-01 1.32e-05
WFG4	9.998e-03 5.92e-04 ≈	1.019e-02 4.81e-04 -	9.943e-03 2.68e-04 ≈	9.993e-03 3.21e-04
WFG5	6.669e-02 3.68e-04 -	6.826e-02 2.06e-03 -	6.645e-02 2.72e-04 ≈	6.640e-02 2.13e-04
WFG6	1.298e-02 3.15e-03 -	1.176e-02 3.80e-04 ≈	1.187e-02 6.78e-04 ≈	1.183e-02 3.42e-04
WFG7	3.253e-02 2.12e-02 -	1.093e-02 1.10e-03 -	1.132e-02 4.14e-04 -	1.066e-02 5.95e-04
WFG8	4.822e-02 1.13e-02 -	3.912e-02 5.54e-03 ≈	4.752e-02 8.24e-03 -	3.787e-02 7.32e-03
WFG9	1.216e-02 1.20e-03 -	1.317e-02 1.94e-03 -	1.166e-02 4.74e-04 ≈	1.168e-02 3.33e-04
DTLZ1	3.304e-02 2.73e-01 -	3.428e+00 6.12e+00 -	1.966e-02 2.72e-04 ≈	1.966e-02 8.87e-04
DTLZ2	7.393e-02 1.25e-03 ≈	7.429e-02 1.58e-03 ≈	7.390e-02 1.18e-03 ≈	7.421e-02 9.71e-04
DTLZ3	8.922e-01 1.22e+00 -	6.568e+00 1.84e+01 -	7.258e-02 2.34e-03 ≈	7.312e-02 3.37e-03
DTLZ4	4.531e-02 1.14e-01 ≈	4.474e-02 2.20e-03 ≈	4.522e-02 2.17e-03 ≈	4.543e-02 2.42e-03
DTLZ5	4.928e-03 1.51e-04 ≈	4.920e-03 1.84e-04 ≈	4.911e-03 9.74e-05 ≈	4.964e-03 2.02e-04
DTLZ6	2.923e-02 3.37e-02 -	4.784e-03 2.65e-04 ≈	4.862e-03 2.54e-04 ≈	4.834e-03 3.13e-04
DTLZ7	1.540e-01 6.42e-03 -	1.419e-01 1.02e-02 +	1.490e-01 5.86e-03 ≈	1.489e-01 2.29e-03
UF1	1.142e-01 6.09e-02 -	8.524e-02 2.54e-02 ≈	9.739e-02 1.70e-02 ≈	9.426e-02 1.44e-02
UF2	5.143e-02 7.92e-03 -	6.054e-02 1.01e-02 -	4.060e-02 8.24e-03 ≈	3.782e-02 6.52e-03
UF3	2.359e-01 5.36e-02 +	2.299e-01 3.11e-02 +	3.258e-01 4.52e-02 ≈	3.264e-01 4.44e-02
UF4	5.998e-02 6.01e-03 -	8.023e-02 1.37e-02 -	4.955e-02 5.28e-03 -	4.584e-02 2.33e-03
UF5	4.231e-01 1.44e-01 -	1.589e+00 4.43e-01 -	3.413e-01 1.54e-01 ≈	3.102e-01 1.57e-01
UF6	3.055e-01 1.90e-01 -	5.960e-01 2.14e-01 -	2.950e-01 1.74e-01 -	1.819e-01 2.16e-01
UF7	2.691e-01 2.66e-01 -	5.024e-02 1.16e-02 ≈	5.282e-02 1.46e-01 ≈	4.711e-02 1.24e-02
UF8	2.927e-01 6.37e-02 -	2.364e-01 2.45e-02 -	1.905e-01 7.80e-03 +	2.084e-01 2.58e-02
UF9	2.550e-01 1.04e-01 ≈	3.059e-01 9.80e-02 -	2.153e-01 9.88e-02 ≈	2.235e-01 1.02e-01
UF10	3.672e-01 1.37e-01 ≈	3.089e+00 2.87e-01 -	5.751e-01 2.41e-01 -	2.937e-01 1.89e-01
-/+≈	20/1/10	18/4/9	7/4/20	-/-

The symbols of “-”, “+” and “≈” denote the corresponding value is significantly worse than, better than, and similar to that of SMS-EMOA-AHX according to the Wilcoxon's rank sum test with the 5% significance level, respectively.

339 ZDT6, DTLZ6, and DTLZ7. Based on these experimental results, it is convincible to conclude that our proposed AHX operator
340 is better than SBX, DE and HBX operators when they are all embedded into NSGA-II.

341 (2) The comparison of the four evolutionary operators in SPEA2

342 **Tables 5** and **6** respectively give the experimental results of the IGD and HV metrics for SPEA2-SBX, SPEA2-DE, SPEA2-
343 HBX, and SPEA2-AHX. The best results of IGD metric in the **Table 5** are highlighted by dark grey background, where it can
344 be observed that SPEA2-AHX performs best on 23 out of 31 test problems in all compared algorithms. Moreover, SPEA2-
345 AHX performs similarly with or outperforms SPEA2-SBX and SPEA2-DE on 29 out of 31 test instances. SPEA2-SBX only beats
346 SPEA2-AHX on WFG4 and UF3, while SPEA2-DE outperforms SPEA2-AHX on WFG2 and UF3. Regarding to the HV metric in
347 **Table 6**, it is found that SPEA2-AHX performs best on 21 out of 31 test problems in all the compared algorithms. Moreover,
348 SPEA2-AHX is better than or similar with SPEA2-SBX and SPEA2-DE, on 31 and 30 out of 31 test instances, respectively.
349 SPEA2-DE only performs better than SPEA2-AHX on UF3. According to the above experimental analysis, it is able to conclude
350 that AHX can significantly enhance the performance of SPEA2 when it is embedded into SPEA2 as a recombination operator.
351 It is interesting to note that AHX seems especially effective for SPEA2. This is mainly because SPEA2 can well maintain the
352 population diversity due to its diversity estimation technique based on clustering. This good population diversity in SPEA2
353 can effectively cooperate with the strong search capability in AHX for enhancing the performance. This fact is also found in
354 [37] that JGBL is especially effective when it is incorporated into SPEA2.

355 Considering the effectiveness of adaptive parameter control in AHX, it can be found out from the comparison of SPEA2-
356 HBX and SPEA2-AHX. When compared to SPEA2-HBX, SPEA2-AHX performs better or similarly on 29 and 30 out of 31 test
357 problems, respectively on the IGD and HV metrics. This indicates that the proposed adaptive parameter control approach
358 also can further improve the performance of SPEA2 when it is cooperated with HBX operator.

Table 8

HV Comparison (Median and IQR) of SMS-EMOA with different variance.

Problems	SMS-EMOA-SBX \tilde{x} IQR	SMS-EMOA-DE \tilde{x} IQR	SMS-EMOA-HBX \tilde{x} IQR	SMS-EMOA-AHX \tilde{x} IQR
ZDT1	3.6617 $1.99e-04$ –	3.1663 $1.54e-01$ –	3.6621 $1.17e-05$ +	3.6620 $2.87e-05$
ZDT2	3.3279 $6.63e-04$ –	2.3299 $5.24e-01$ –	3.3288 $2.57e-05$ +	3.3287 $2.75e-05$
ZDT3	4.8150 $1.21e-04$ –	3.7293 $5.89e-01$ –	4.8155 $4.63e-05$ ≈	4.8155 $1.19e-04$
ZDT4	3.5737 $9.92e-02$ –	0.0000 $0.00e+00$ –	3.6619 $1.37e-04$ +	3.6548 $6.09e-02$
ZDT6	3.0335 $2.25e-03$ –	3.0419 $1.53e-05$ ≈	3.0419 $1.10e-05$ ≈	3.0419 $1.13e-05$
WFG1	3.7765 $2.36e+00$ –	12.014 $1.15e-01$ –	12.074 $3.30e-03$ –	12.074 $7.87e-04$
WFG2	10.589 $1.34e+00$ –	11.462 $8.35e-01$ ≈	10.626 $7.31e-04$ –	10.627 $7.74e-05$
WFG3	10.683 $1.20e-01$ –	10.959 $4.53e-05$ +	10.959 $2.02e-04$ –	10.959 $5.50e-05$
WFG4	8.1743 $2.00e-01$ –	8.4825 $5.44e-02$ –	8.5724 $6.40e-02$ –	8.5961 $4.45e-02$
WFG5	7.9060 $6.67e-02$ –	7.7068 $1.39e-01$ –	7.9882 $7.96e-02$ –	8.0575 $4.90e-02$
WFG6	8.2611 $2.59e-01$ –	8.6877 $1.64e-03$ ≈	8.6843 $2.46e-01$ –	8.6880 $3.82e-04$
WFG7	6.9656 $3.52e-01$ –	8.6699 $7.80e-01$ ≈	8.3081 $3.85e-02$ –	8.6878 $3.71e-01$
WFG8	7.4895 $2.58e-01$ –	7.6508 $1.67e-01$ –	8.0274 $1.26e-01$ –	8.1648 $1.30e-01$
WFG9	8.2533 $8.59e-02$ –	8.2120 $1.01e-01$ –	8.3287 $6.06e-02$ ≈	8.3528 $5.59e-02$
DTLZ1	0.9670 $1.87e-01$ –	0.0000 $0.00e+00$ –	0.9738 $2.15e-04$ ≈	0.9738 $4.58e-04$
DTLZ2	7.4267 $2.49e-04$ –	7.4261 $2.01e-04$ –	7.4269 $5.54e-05$ ≈	7.4269 $7.78e-05$
DTLZ3	3.8228 $7.13e+00$ –	0.0000 $2.56e+00$ –	7.4244 $1.48e-03$ +	7.4192 $9.50e-03$
DTLZ4	7.4267 $1.00e+00$ ≈	7.4246 $6.57e-04$ –	7.4268 $5.89e-05$ ≈	7.4268 $5.78e-05$
DTLZ5	6.1041 $5.79e-05$ ≈	6.1040 $2.95e-05$ –	6.1041 $2.30e-05$ +	6.1041 $2.86e-05$
DTLZ6	6.0418 $1.09e-01$ –	6.1041 $3.73e-05$ +	6.1041 $2.63e-05$ ≈	6.1041 $4.43e-05$
DTLZ7	13.441 $1.84e-02$ –	13.363 $5.62e-02$ –	13.459 $1.82e-02$ ≈	13.459 $6.26e-04$
UF1	3.2977 $1.29e-01$ –	3.4836 $1.16e-01$ –	3.3337 $1.65e-01$ –	3.5157 $1.14e-02$
UF2	3.4762 $7.86e-02$ –	3.5232 $4.60e-02$ –	3.5371 $6.54e-02$ –	3.5959 $4.73e-02$
UF3	2.6067 $9.22e-02$ –	3.3031 $4.77e-02$ +	2.8211 $7.86e-02$ –	2.9918 $3.43e-01$
UF4	3.1724 $7.89e-03$ –	3.1037 $3.23e-02$ –	3.2030 $5.59e-03$ –	3.2077 $5.18e-03$
UF5	1.9544 $4.08e-01$ –	0.1302 $3.55e-01$ –	2.3128 $7.64e-01$ –	2.7991 $5.79e-01$
UF6	2.5819 $6.08e-01$ –	1.8015 $2.96e-01$ –	2.5964 $6.64e-01$ –	2.9872 $6.79e-01$
UF7	2.6281 $7.39e-01$ –	3.3776 $3.86e-02$ –	3.2978 $2.97e-01$ –	3.4231 $7.21e-02$
UF8	6.4189 $1.64e-02$ +	6.1093 $2.07e-01$ –	6.4049 $5.54e-03$ –	6.4132 $2.24e-03$
UF9	5.7966 $8.80e-01$ –	6.2285 $7.91e-01$ –	6.7478 $6.84e-01$ ≈	6.7871 $7.32e-01$
UF10	4.9594 $2.35e+00$ ≈	0.0000 $0.00e+00$ –	4.0619 $1.18e+00$ –	5.8350 $2.23e+00$
–/+/≈	27/1/3	24/3/4	17/5/9	–/-/–

The symbols of “–”, “+” and “≈” denote the corresponding value is significantly worse than, better than, and similar to that of SMS-EMOA-AHX according to the Wilcoxon's rank sum test with the 5% significance level, respectively.

(3) The comparison of the four evolutionary operators in SMS-EMOA

The IGD and HV results of SMS-EMOA with different crossover operators are illustrated in Tables 7 and 8, respectively. For the IGD metric in Table 7, although the advantage of SMS-EMOA-AHX is not as obvious as that of NSGA-II-AHX and SPEA2-AHX, the proposed AHX operator still improves the performance of SMS-EMOA on most of the test problems. Especially, SMS-EMOA-AHX achieves the best values on 12 test problems and the second best values on 13 test problems when compared to SMS-EMOA-SBX, SMS-EMOA-DE and SMS-EMOA-HBX. Moreover, SMS-EMOA-AHX performs better than or similarly with SMS-EMOA-SBX on 30 out of 31 test problems, and better than or similarly with SMS-EMOA-DE on 27 out of 31 test problems. These experimental results validate the advantage of AHX when it is embedded into SMS-EMOA.

When considering the HV metric in Table 8, similar results on the IGD metric are observed. SMS-EMOA-AHX achieves the best results on 17 test problems and the second best results on 13 test problems. In other words, SME-EMOA-AHX performs best or secondly best on 30 out of 31 test problems when compared with SMS-EMOA-SBX, SMS-EMOA-DE and SMS-EMOA-HBX. Note that the degree of performance improvement brought by AHX is considerable on some test problems, such as ZDT4, DTLZ1, DTLZ3, UF2, and UF4–UF6.

Based on the above analysis, it is reasonable to conclude that the performance of our proposed AHX operator is better than SBX and DE when it is embedded into the framework of SMS-EMOA, and our proposed adaptive parameter control approach is also effective to further enhance the performance.

(4) The comparison of the four evolutionary operators in MOEA/D

Our proposed operator AHX is further embedded into MOEA/D and the experimental results of MOEA/D-SBX [65], MOEA/D-DE [40], MOEA/D-HBX, and MOEA/D-AHX are shown in Tables 9 and 10. It is observed that the proposed AHX operator can improve the performance of MOEA/D in most of the test problems.

Table 9

IGD Comparison (Median and IQR) of MOEA/D with different variance.

Problems	MOEA/D-SBX \tilde{x}_{IQR}	MOEA/D-DE \tilde{x}_{IQR}	MOEA/D-HBX \tilde{x}_{IQR}	MOEA/D-AHX \tilde{x}_{IQR}
ZDT1	4.404e-03 7.97e-05 –	1.297e-02 5.07e-03 –	4.294e-03 2.01e-05 +	4.324e-03 3.48e-05
ZDT2	4.282e-03 7.67e-05 –	1.006e-02 4.13e-03 –	4.212e-03 1.57e-05 +	4.225e-03 2.09e-05
ZDT3	1.166e-02 7.88e-05 +	4.382e-02 1.80e-02 –	1.168e-02 1.66e-04 ≈	1.174e-02 1.11e-04
ZDT4	7.575e-03 2.59e-03 –	1.774e-01 2.96e-01 –	4.346e-03 8.30e-05 +	5.733e-03 1.22e-03
ZDT6	5.672e-03 8.44e-04 –	2.317e-03 1.32e-05 ≈	2.319e-03 5.95e-06 ≈	2.319e-03 8.94e-06
WFG1	1.734e+00 1.53e-01 –	4.659e-02 4.62e-02 –	2.482e-02 1.78e-03 ≈	2.474e-02 1.06e-02
WFG2	2.573e-01 5.63e-03 –	8.935e-02 8.41e-03 –	9.146e-02 1.58e-01 –	8.636e-02 3.44e-02
WFG3	4.062e-01 1.81e-02 –	3.849e-01 5.65e-05 ≈	3.849e-01 8.27e-05 ≈	3.849e-01 4.62e-05
WFG4	1.724e-02 6.76e-04 ≈	1.844e-02 1.99e-03 –	1.735e-02 1.27e-03 ≈	1.734e-02 1.72e-03
WFG5	6.780e-02 3.91e-04 –	6.744e-02 1.91e-04 –	6.741e-02 1.78e-04 ≈	6.740e-02 1.71e-04
WFG6	2.000e-02 7.70e-03 –	1.922e-02 4.26e-03 ≈	1.710e-02 2.54e-03 ≈	1.712e-02 3.27e-03
WFG7	1.794e-02 1.98e-03 +	1.809e-02 1.03e-03 +	1.880e-02 6.14e-04 –	1.863e-02 5.56e-04
WFG8	7.681e-02 2.23e-02 –	2.525e-02 3.40e-03 +	5.904e-02 1.55e-02 –	4.450e-02 8.91e-03
WFG9	1.658e-02 9.91e-04 –	1.632e-02 5.19e-04 –	1.595e-02 2.27e-04 ≈	1.599e-02 8.69e-05
DTLZ1	3.397e-02 2.49e-02 –	4.419e-02 1.65e+00 –	6.744e-02 3.09e-03 –	3.192e-02 7.31e-04
DTLZ2	7.305e-02 4.83e-04 +	7.393e-02 7.10e-04 –	1.877e-01 3.95e-03 –	7.335e-02 6.56e-04
DTLZ3	8.138e-02 1.73e-02 –	8.947e-02 4.23e-01 –	2.144e-01 5.32e-03 –	7.548e-02 2.95e-03
DTLZ4	8.107e-02 8.08e-02 ≈	5.979e-02 7.64e-03 +	6.117e-02 1.83e-03 +	8.024e-02 2.42e-03
DTLZ5	1.491e-02 1.16e-05 ≈	1.471e-02 9.26e-05 +	8.329e-03 2.22e-05 +	1.490e-02 1.57e-05
DTLZ6	2.845e-02 3.29e-02 –	1.402e-02 4.28e-05 +	8.258e-03 1.65e-05 +	1.409e-02 2.24e-05
DTLZ7	1.995e-01 1.42e-02 –	1.853e-01 2.44e-02 ≈	3.872e-01 2.47e-03 –	1.868e-01 1.44e-02
UF1	1.609e-01 9.01e-02 –	8.267e-02 2.19e-02 ≈	7.905e-02 3.34e-02 –	6.829e-02 1.02e-02
UF2	5.522e-02 3.41e-02 –	3.815e-02 1.51e-02 ≈	4.056e-02 5.93e-03 –	3.705e-02 5.80e-03
UF3	2.943e-01 3.40e-02 ≈	1.647e-01 7.50e-02 +	2.937e-01 2.03e-02 ≈	2.989e-01 4.18e-02
UF4	6.412e-02 4.13e-03 –	9.332e-02 1.29e-02 –	5.778e-02 1.02e-02 –	5.166e-02 5.62e-03
UF5	5.053e-01 2.07e-01 ≈	9.926e-01 2.48e-01 –	3.879e-01 1.63e-01 ≈	4.129e-01 3.32e-01
UF6	4.271e-01 3.11e-01 ≈	3.882e-01 1.34e-01 ≈	4.452e-01 2.44e-01 ≈	4.415e-01 4.11e-01
UF7	3.534e-01 2.12e-01 –	3.348e-02 1.96e-02 +	4.017e-02 1.98e-02 ≈	3.718e-02 1.57e-02
UF8	2.417e-01 4.97e-02 +	2.203e-01 2.06e-02 +	3.914e-01 2.63e-02 –	2.549e-01 3.86e-02
UF9	2.864e-01 7.00e-02 –	2.184e-01 7.04e-02 ≈	3.655e-01 6.54e-02 –	2.179e-01 2.11e-02
UF10	5.186e-01 2.16e-01 –	1.108e+00 2.47e-01 –	7.502e-01 1.40e-01 –	4.221e-01 2.36e-01
-/+/≈	21/4/6	15/8/8	13/6/12	-/-/-

The symbols of “–”, “+” and “≈” denote the corresponding value is significantly worse than, better than, and similar to that of MOEA/D-AHX according to the Wilcoxon's rank sum test with the 5% significance level, respectively.

379 Regarding to the IGD metric in **Table 9**, MOEA/D-AHX outperforms MOEA/D-SBX, MOEA/D-DE and MOEA/D-HBX in 21,
380 15 and 13 out of 31 test problems, respectively. The Wilcoxon rank sum test indicates that MOEA/D-AHX obtains the statis-
381 tically similar results with MOEA/D-SBX on 6 test problems, with MOEA/D-DE on 8 test problems, and MOEA/D-HBX on 12
382 test problems. In contrast, MOEA/D-SBX, MOEA/D-DE and MOEA/D-HBX only outperform MOEA/D-AHX on 5, 8 and 6 test
383 problems, respectively.

384 Considering the HV metric in **Table 10**, MOEA/D-AHX outperforms MOEA/D-SBX, MOEA/D-DE and MOEA/D-HBX in 26,
385 21 and 16 out of 31 test problems. The Wilcoxon rank sum test indicates that MOEA/D-AHX obtains the statistically similar
386 results with MOEA/D-SBX on 5 test problems, with MOEA/D-DE on 6 test problems, and with MOEA/D-HBX on 12 test
387 problems. In contrast, MOEA/D-AHX only underperforms MOEA/D-SBX, MOEA/D-DE and MOEA/D-HBX on 0, 4 and 3 test
388 problems, respectively.

389 Based on the above analysis, it is obvious that our proposed AHX operator performs better than SBX and DE operators
390 when it is embedded into MOEA/D on both the IGD and HV metrics. Moreover, the effectiveness of adaptive parameter
391 control approach is also confirmed from the comparison of MEOA/D-HBX and MOEA/D-AHX.

392 At last, in **Table 11**, the comparison results of the four MOEA frameworks (NSGA-II, SPEA2, SMS-EMOA, MOEA/D) with
393 different crossover operators (i.e. SBX and DE) on the IGD and HV metrics are summarized to evaluate the comprehensive
394 performance in solving all the test problems. The comparison results are represented as “b/w/s”, which means that AHX
395 is respectively better than, worse than and equal to the corresponding competitor on b, w and s test problems. From the
396 last row of **Table 11**, the total numbers of the test problems that AHX performs better than, worse than and similar to SBX
397 with statistical significance are 79/11/34 and 104/3/17 regarding to IGD and HV metrics, respectively. When compared to DE,
398 AHX performs better than, worse than and similar to DE on 81/18/25 test problems on the IGD metric, and 99/11/14 test

Table 10

HV Comparison (Median and IQR) of MOEA/D with different variance.

Problems	MOEA/D-SBX \tilde{x} IQR	MOEA/D-DE \tilde{x} IQR	MOEA/D-HBX \tilde{x} IQR	MOEA/D-AHX \tilde{x} IQR
ZDT1	3.6590 7.76e-04 –	3.6300 1.06e-02 –	3.6604 1.28e-04 ≈	3.6604 2.45e-04
ZDT2	3.3249 1.44e-03 –	3.2833 2.23e-02 –	3.3275 2.33e-04 ≈	3.3275 2.06e-04
ZDT3	4.8093 8.02e-04 –	4.6576 6.53e-02 –	4.8112 9.84e-05 ≈	4.8112 1.54e-04
ZDT4	3.6450 8.39e-03 –	3.1554 9.18e-01 –	3.6601 3.46e-04 +	3.6541 5.37e-03
ZDT6	3.0288 2.92e-03 –	3.0413 1.28e-05 ≈	3.0413 1.20e-05 ≈	3.0413 1.34e-05
WFG1	3.9562 1.42e-00 –	11.934 2.21e-01 –	12.045 1.54e-02 ≈	12.051 4.93e-02
WFG2	9.2429 3.17e-02 –	10.596 4.70e-02 –	10.602 1.33e+00 –	10.615 7.98e-01
WFG3	10.696 1.63e-01 –	10.944 3.24e-03 –	10.944 2.59e-03 –	10.946 1.61e-03
WFG4	8.5064 6.44e-02 –	8.4389 5.09e-02 –	8.5155 5.41e-02 –	8.5405 4.88e-02
WFG5	8.0069 5.66e-02 –	8.0440 1.79e-02 –	8.0390 3.16e-02 ≈	8.0505 2.33e-02
WFG6	8.2604 2.16e-01 –	8.3194 4.32e-01 ≈	8.6639 3.95e-01 ≈	8.6382 4.07e-01
WFG7	7.7627 2.36e-01 –	8.2822 1.15e+00 ≈	8.2595 3.19e-02 –	8.2760 3.02e-02
WFG8	7.8315 1.71e-01 –	8.2558 8.18e-02 +	7.9542 1.78e-01 –	8.1931 9.48e-02
WFG9	8.2600 9.63e-02 –	8.3080 3.29e-02 –	8.3393 2.70e-02 –	8.3538 3.20e-02
DTLZ1	0.9647 1.90e-02 –	0.9556 9.65e-01 –	0.9558 9.41e-04 –	0.9676 6.85e-04
DTLZ2	7.3698 1.11e-03 –	7.3709 3.12e-03 ≈	7.3018 1.49e-03 –	7.3716 1.95e-03
DTLZ3	7.3518 4.20e-02 –	7.3091 2.93e+00 –	7.3038 3.04e-03 –	7.3776 4.44e-03
DTLZ4	7.3718 9.67e-01 –	7.3767 5.47e-03 +	7.3028 1.39e-03 –	7.3750 2.85e-03
DTLZ5	6.0841 1.77e-04 ≈	6.0836 2.83e-04 –	6.0960 3.23e-05 +	6.0843 3.04e-04
DTLZ6	6.0259 8.49e-02 –	6.0840 1.64e-04 +	6.0958 2.63e-04 +	6.0839 3.30e-05
DTLZ7	13.254 2.39e-03 ≈	13.224 2.89e-02 –	11.303 8.59e-03 –	13.255 2.09e-03
UF1	3.1091 2.13e-01 –	3.3944 1.96e-01 –	3.3455 2.72e-01 –	3.5277 1.62e-01
UF2	3.4584 1.19e-01 –	3.4930 9.68e-02 –	3.5575 6.89e-02 ≈	3.5554 8.52e-02
UF3	2.5187 4.75e-02 –	3.1207 6.01e-01 +	2.5689 4.63e-02 –	2.8524 1.15e-01
UF4	3.1245 1.82e-02 –	3.0567 5.01e-02 –	3.1911 1.53e-02 –	3.1997 1.14e-02
UF5	1.8194 4.54e-01 –	0.8929 3.67e-01 –	2.1374 3.57e-01 ≈	2.0285 9.34e-01
UF6	2.2031 3.56e-01 ≈	2.2470 3.75e-01 ≈	2.2209 3.36e-01 ≈	2.1866 9.52e-01
UF7	2.4818 4.29e-01 –	3.3522 1.82e-01 –	3.3758 1.95e-01 ≈	3.4299 1.93e-01
UF8	6.3933 1.34e-02 ≈	6.0290 2.24e-01 –	6.3526 1.71e-02 –	6.3976 7.19e-03
UF9	5.6297 5.79e-01 –	6.6156 5.65e-01 ≈	6.1013 3.69e-01 –	6.6101 5.85e-01
UF10	3.5863 7.35e-01 ≈	1.2105 5.50e-01 –	3.9508 2.53e-01 ≈	3.7174 2.81e+00
–/+/≈	26/0/5	21/4/6	16/3/12	–/-/-

The symbols of “–”, “+” and “≈” denote the corresponding value is significantly worse than, better than, and similar to that of MOEA/D-AHX according to the Wilcoxon's rank sum test with the 5% significance level, respectively.

Table 11

Final results of SBX, DE, and HBX compared with AHX in NSGA-II, SPEA2, SMS-EMOA, and MOEA/D.

IGD	HV						
	Operators	SBX	DE	HBX			
NSGA-II	17/4/10	22/4/5	9/5/17	NSGA-II	24/2/5	26/3/2	19/3/9
SPEA2	21/2/8	26/2/3	14/2/15	SPEA2	27/0/4	28/1/2	21/1/9
SMS-EMOA	20/1/10	18/4/9	7/4/20	SMS-EMOA	27/1/3	24/3/4	17/5/9
MOEA/D	21/4/6	15/8/8	13/6/12	MOEA/D	26/0/5	21/4/6	16/3/12
Total (b/w/s)	79/11/34	81/18/25	43/17/64	Total (b/w/s)	104/3/17	99/11/14	73/12/39

“b/w/s” denote that AHX is significantly better than, worse than and similar to the corresponding competitor on b, w and s functions, respectively.

problems on the HV metric. It is clear that our proposed AHX operator can significantly improve the performance of MOEAs when compared to SBX and DE operators. Regarding the comparison of AHX with HBX, although the Wilcoxon rank sum test shows that AHX has 64 test problems similar to HBX, AHX still performs better than HBX on 43 test problems for the IGD metric. Moreover, AHX is better than, worse than and similar to HBX on 73, 12, 39 test problems for the HV metric. These experimental results validate that our adaptive parameters control method is able to improve the comprehensive performance of HBX.

Table 12

HV and IGD Comparison (Median and IQR) of imade with different variance.

Problems	IMADE \tilde{x}_{IQR} (IGD)	IMA-AHX \tilde{x}_{IQR} (IGD)	IMADE \tilde{x}_{IQR} (HV)	IMA-AHX \tilde{x}_{IQR} (HV)
ZDT1	3.847e-03 7.18e-05 –	3.747e-03 3.55e-05	3.66155 1.39e-04 –	3.66185 8.47e-05
ZDT2	3.914e-03 7.20e-05 –	3.881e-03 4.85e-05	3.32846 1.25e-04 –	3.32859 9.77e-05
ZDT3	4.437e-03 9.79e-05 ≈	4.423e-03 7.06e-05	4.81533 6.37e-05 ≈	4.81530 7.64e-05
ZDT4	4.563e-03 5.27e-04 –	3.962e-03 4.15e-04	3.65837 1.74e-03 –	3.66054 2.27e-03
ZDT6	2.813e-03 1.88e-04 ≈	2.798e-03 1.15e-04	3.04183 3.45e-05 –	3.04187 4.47e-05
WFG1	1.224e-02 2.99e-04 +	1.248e-02 8.07e-03	12.0724 3.47e-04 +	12.0713 3.26e-02
WFG2	6.478e-02 8.63e-04 ≈	6.488e-02 6.26e-04	10.6260 9.78e-04 ≈	10.6260 8.82e-04
WFG3	3.832e-01 1.98e-04 –	3.831e-01 1.22e-04	10.9508 2.20e-03 –	10.9533 3.37e-03
WFG4	1.127e-02 4.22e-04 –	1.080e-02 4.40e-04	8.64269 2.35e-02 +	8.61832 2.44e-02
WFG5	6.648e-02 1.93e-04 ≈	6.647e-02 2.86e-04	8.11510 1.31e-02 +	8.09442 2.49e-02
WFG6	1.320e-02 5.31e-04 ≈	1.307e-02 1.42e-03	8.67898 1.86e-01 ≈	8.57260 3.14e-01
WFG7	1.258e-02 4.90e-04 ≈	1.244e-02 5.33e-04	8.68148 3.28e-01 +	8.31656 1.87e-02
WFG8	2.096e-02 1.65e-03 +	2.808e-02 2.42e-03	8.40689 4.54e-02 +	8.33974 8.39e-02
WFG9	1.282e-02 2.68e-04 –	1.251e-02 3.07e-04	8.36270 3.61e-02 ≈	8.36478 3.60e-02
DTLZ1	8.857e-01 1.86e+00 –	2.856e-02 1.03e-02	0.03001 5.11e-01 –	0.96802 5.28e-03
DTLZ2	6.844e-02 3.54e-03 –	6.543e-02 3.50e-03	7.37584 6.04e-03 –	7.38352 3.05e-03
DTLZ3	2.228e+00 4.31e+00 –	7.534e-02 2.02e-02	0.00000 2.84e+00 –	7.34764 8.38e-02
DTLZ4	6.612e-02 6.85e-03 –	5.992e-02 6.45e-03	7.37708 6.63e-03 –	7.38957 3.85e-03
DTLZ5	4.369e-03 1.94e-04 –	4.143e-03 1.13e-04	6.10124 3.96e-04 –	6.10298 2.75e-04
DTLZ6	3.990e-03 2.41e-04 ≈	3.927e-03 2.40e-04	6.10353 7.57e-05 ≈	6.10356 5.15e-05
DTLZ7	7.726e-02 5.57e-03 ≈	7.563e-02 4.99e-03	13.3385 7.38e-02 ≈	13.3389 7.48e-02
UF1	7.515e-02 8.72e-03 +	8.345e-02 2.28e-02	3.41068 1.26e-01 ≈	3.42872 2.15e-01
UF2	4.682e-02 7.42e-03 –	4.078e-02 5.14e-03	3.55683 7.36e-02 ≈	3.56174 7.75e-02
UF3	2.567e-01 6.15e-02 +	3.134e-01 7.10e-02	3.08031 1.32e-01 ≈	3.03121 2.41e-01
UF4	4.892e-02 2.70e-03 +	5.081e-02 2.48e-03	3.20563 4.05e-03 +	3.20211 5.38e-03
UF5	4.548e-01 2.98e-01 +	5.944e-01 1.52e-01	2.07405 5.69e-01 +	1.68886 4.34e-01
UF6	3.481e-01 4.82e-02 ≈	3.558e-01 7.78e-02	2.45039 3.48e-01 ≈	2.21291 2.94e-01
UF7	8.260e-02 1.89e-01 ≈	4.788e-02 2.02e-01	3.34225 7.99e-01 ≈	3.37422 7.73e-01
UF8	1.086e+00 8.05e-01 –	3.234e-01 1.72e-01	1.44536 2.20e+00 –	5.75875 8.80e-01
UF9	1.113e+00 6.21e-01 –	6.526e-01 2.40e-01	1.58499 1.90e+00 –	4.42103 1.93e+00
UF10	3.845e+00 2.99e+00 –	2.033e+00 1.28e+00	0.00000 0.00e+00 –	0.02389 5.60e-01
–/+/≈	15/6/10	–/–/–	13/7/11	–/–/–

The symbols of “–”, “+” and “≈” denote the corresponding value is significantly worse than, better than, and similar to that of IMA-AHX according to the Wilcoxon's rank sum test with the 5% significance level, respectively.

4.4.2. The comparison of IMADE and IMA-AHX

In IMADE, a recombination operator DEI simply combining the SBX and DE operators is designed and further embedded into a multiobjective immune algorithm. The difference of DEI and AHX is clearly described in Section 1 and this subsection gives the experimental comparison between the two recombination operators.

The experimental results of 31 test problems using the IGD and HV metrics are listed in Table 12. Clearly, IMA-AHX performs significantly better than IMADE in both metrics as IMA-AHX obtains the better results on 15 and 13 out of 31 test problems regarding to the IGD and HV metrics, respectively. The Wilcoxon rank sum test indicates that IMA-AHX performs similarly with IMADE on 10 and 11 test problems, respectively for the IGD and HV metrics. Overall, IMA-AHX performs better than or similarly to IMADE on 25 and 24 out of 31 test problems respectively for the IGD and HV metrics. Moreover, it is worth noting that the improvement of IMA-AHX is significant for some cases, such as DTLZ1 and DTLZ3. Therefore, the proposed AHX operator in this paper is experimentally validated to perform better than DEI operator in IMADE. This also confirms our viewpoint that the gene-level based AHX is better than the chromosome-level based DEI, although they all combine the merits of SBX and DE.

4.5. Further comparison and analysis

4.5.1. The comparison of AHX, JGBL and FRRMAB

In this subsection, AHX is further compared with two recently proposed hybrid crossover operators, i.e., JGBL and FRRMAB. Following the original reference, JGBL [37] is implemented in the framework of SPEA2, named SPEA2-JGBL, while FRRMAB [34] is embedded into MOEA/D, named MOEA/D-FRRMAB. To have a fair comparison, AHX is also implemented in

Table 13

IGD Comparison (Median and IQR) of AHX, JGBL and FRRMAB.

Problems	SPEA2-JGBL \tilde{x} IQR	SPEA2-AHX \tilde{x} IQR	MOEA/D-FRRMAB \tilde{x} IQR	MOEA/D-AHX \tilde{x} IQR
ZDT1	5.039e−03 3.79e−04 −	3.901e−03 7.81e−05	3.815e−02 1.20e−02 −	4.013e−03 7.21e−05
ZDT2	5.033e−03 3.88e−04 −	3.903e−03 6.36e−05	2.507e−02 9.14e−03 −	3.906e−03 4.89e−05
ZDT3	5.469e−03 2.56e−04 −	4.766e−03 1.78e−04	8.428e−02 4.49e−02 −	1.070e−02 5.39e−05
ZDT4	3.949e−03 7.62e−05 +	9.674e−03 9.77e−03	9.899e−01 9.08e−01 −	7.754e−03 5.89e−03
ZDT6	1.452e−02 2.11e−03 −	2.280e−03 1.56e−04	1.907e−03 1.50e−05 ∼	1.907e−03 8.13e−06
DTLZ1(3)	7.720e−02 1.97e−01 −	2.627e−02 1.51e−02	3.287e−02 1.55e−01 −	2.961e−02 1.10e−03
DTLZ2(3)	6.184e−02 3.61e−03 −	5.428e−02 1.37e−03	6.778e−02 8.42e−04 −	6.718e−02 7.39e−04
DTLZ3(3)	1.797e−01 3.07e−01 −	6.068e−02 1.70e−02	9.932e−02 3.40e−01 −	7.665e−02 1.37e−02
DTLZ4(3)	4.166e−02 1.13e−02 ∼	4.217e−02 5.48e−03	5.045e−02 8.96e−03 +	7.192e−02 2.91e−03
DTLZ5(3)	4.543e−03 2.83e−04 −	4.398e−03 1.85e−04	1.247e−02 1.40e−04 +	1.268e−02 3.30e−05
DTLZ6(3)	5.123e−01 1.20e−01 −	4.055e−03 1.50e−04	1.184e−02 4.16e−05 +	1.195e−02 1.34e−05
DTLZ7(3)	6.791e−02 3.15e−03 −	5.769e−02 1.44e−03	1.887e−01 2.34e−02 +	1.995e−01 1.33e−02
DTLZ1(6)	9.440e+01 1.88e+01 −	9.470e−02 5.31e−03	4.841e−01 6.16e−01 −	1.214e−01 1.79e−05
DTLZ2(6)	7.778e−01 8.65e−02 −	2.810e−01 1.24e−02	3.943e−01 2.00e−02 −	3.559e−01 5.91e−05
DTLZ3(6)	4.057e+02 1.28e+02 −	6.909e+00 3.40e+00	2.038e+00 4.51e+00 −	3.559e−01 1.88e−03
DTLZ4(6)	8.662e−01 1.38e−01 −	3.125e−01 1.51e−02	4.715e−01 3.27e−02 −	3.559e−01 1.05e−04
DTLZ5(6)	5.465e−01 2.14e−01 −	3.035e−01 1.16e−01	4.270e−02 1.97e−04 +	4.403e−02 8.02e−04
DTLZ6(6)	5.494e+00 7.33e−01 −	1.018e+00 6.34e−01	4.276e−02 2.70e−05 ∼	4.275e−02 5.59e−05
DTLZ7(6)	7.244e−01 3.44e−02 −	3.526e−01 1.12e−02	7.415e−01 1.21e−01 −	7.001e−01 6.73e−05
DTLZ1(10)	1.182e+02 2.45e+01 −	1.089e+02 5.97e+01	2.031e−01 9.04e−02 ∼	2.125e−01 2.49e−03
DTLZ2(10)	1.658e+00 1.79e−01 +	2.063e+00 2.60e−01	5.531e−01 3.70e−02 −	5.359e−01 1.80e−03
DTLZ3(10)	9.593e+02 2.20e+02 −	7.668e+02 2.86e+02	7.119e−01 1.41e−01 −	6.163e−01 1.62e−01
DTLZ4(10)	2.216e+00 2.01e−01 −	1.452e+00 5.44e−01	7.208e−01 5.25e−02 −	5.934e−01 6.06e−02
DTLZ5(10)	1.213e+00 1.84e−01 ∼	1.155e+00 5.90e−01	4.800e−02 1.71e−03 +	5.010e−02 6.93e−04
DTLZ6(10)	7.503e+00 3.63e−01 +	9.837e+00 1.05e−01	3.169e−02 8.59e−03 +	4.169e−02 1.16e−02
DTLZ7(10)	1.487e+00 8.60e−02 −	1.287e+00 3.99e−02	1.038e+00 3.26e−02 +	2.532e+00 7.58e−04
−/+/≈	21/3/2	−/−/−	15/8/3	−/−/−

The symbols of “−”, “+” and “≈” denote the corresponding value is significantly worse than, better than, and similar to that of IMA-AHX according to the Wilcoxon's rank sum test with the 5% significance level, respectively.

423 the frameworks of SPEA2 and MOEA/D, called SPEA2-AHX and MOEA/D-AHX. ZDT and DTLZ test problems are used in this
424 comparison. To study the scalability of AHX in solving many-objective optimization problems, DTLZ test problems are ex-
425 tended to have 3, 6, 10 objectives. The population size and archive size are all set to 252 for 6-objective DTLZ test problems
426 and 275 for 10-objective DTLZ test problems. The function evaluations are all set to 100,000 for 6-objective and 10-objective
427 DTLZ test problems. Other parameters settings are the same as mentioned in [Section 4.3](#). All the comparison results of IGD
428 metric are listed on [Table 13](#), where the median \tilde{x} and the interquartile range IQR over 30 independent runs are shown. It
429 is noted that DTLZ1(3) in [Table 13](#) indicates DTLZ1 test problems with 3 objectives.

430 Considering the comparison results of SPEA2-JGBL and SPEA2-AHX in the second and third columns of [Table 13](#), it is
431 observed that SPEA2-AHX respectively performs better than, worse than and similar to SPAE2-JGBL on 21, 3 and 2 out of
432 26 test problems. SPEA2-JGBL only performs better than SPEA2-AHX on ZDT4, DTLZ2(10) and DTLZ6(10). Moreover, it is
433 pointed out that the degree of performance improvement brought by AHX is considerable on some test problems, such
434 as ZDT6, DTLZ1 and DTLZ3. These experimental results validate that our proposed AHX operator is better than the JGBL
435 paradigm in the framework of SPEA2.

436 Regarding the comparison of MOEA/D-AHX and MOEA/D-FRRMAB, the IGD results are illustrated in fourth and fifth
437 columns of [Table 13](#). It is observed that MOEA/D-AHX respectively performs better than, worse than and similar to MOEA/D-
438 FRRMAB on 15, 8 and 3 out of 26 test problems, while MOEA/D-AHX is only worse than MOEA/D-FRRMAB on DTLZ5,
439 DTLZ6 and DTLZ7 with 3 and 10 objectives. Moreover, on some test problems, such as ZDT1-ZDT4, DTLZ1 and DTLZ3,
440 AHX is found to considerably outperform FRRMAB. Therefore, considering all the test problems, it is reasonable to con-
441 clude that AHX is not only better than original DE operator, but also better than FRRMAB (multiple DE operators used in
442 FRRMAB).

443 4.5.2. The influence by the dimensionality of MOPs

444 In this subsection, we further investigate the performance of AHX affected by the dimensionality of MOPs. AHX and SBX
445 are all implemented in the framework of SPEA2 for performance comparison, called SPEA2-AHX and SPEA2-SBX. Four MOPs,
446 i.e., ZDT1, WFG1, DTLZ1 and UF1, including 10, 30 and 50 decision variables, are used to test their optimization performance.

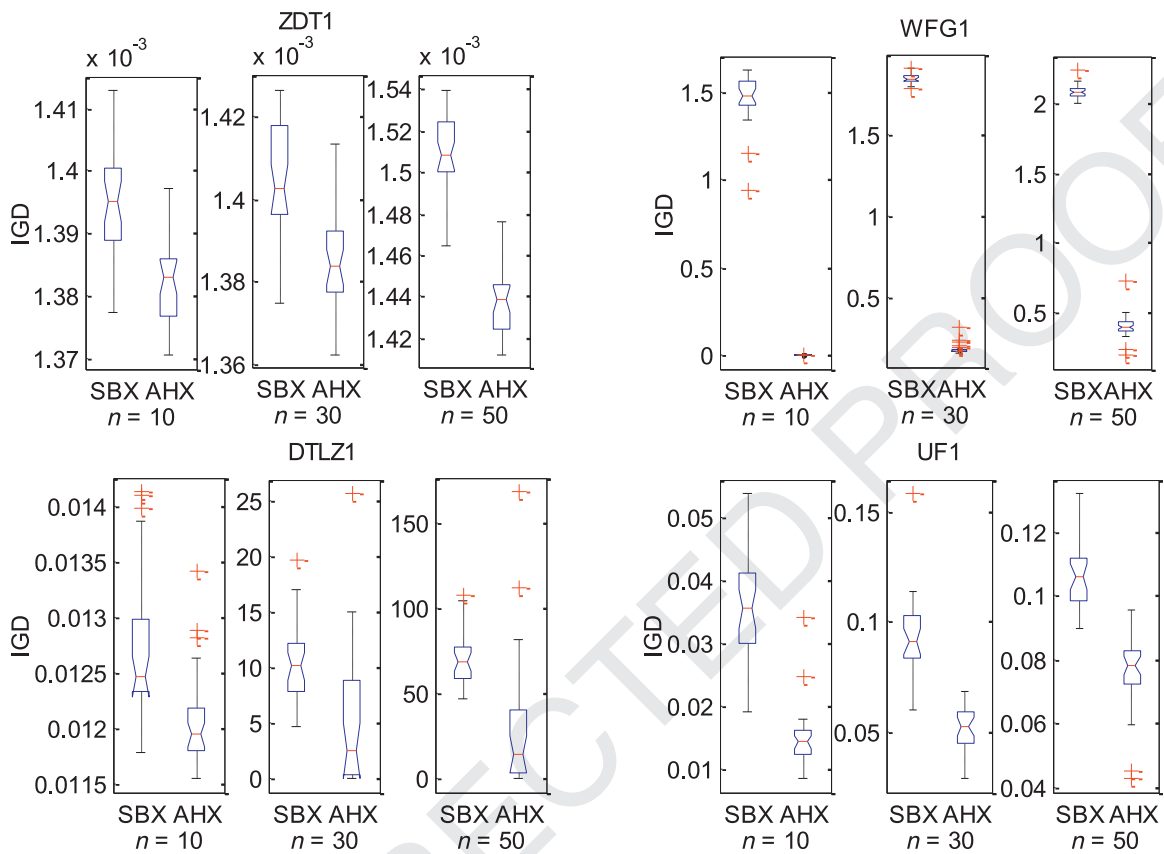


Fig. 7. The comparison of AHX and SBX in the framework of SPEA2 to solve ZDT1, WFG1, DTLZ1 and UF1 with different decision variables n .

447 All the simulations are run by 30 times and their IGD values are all illustrated by the box plots in Fig. 7, where the central
 448 red line indicates the median value, the edges of the box are the 25th and 75th percentiles, and the red symbol "+" denotes
 449 outliers. As the increase of dimensionality in decision space will enhance the difficulty of MOPs, it is observed from Fig. 7
 450 that the performance of SPEA2-AHX and SPEA2-SBX is gradually reduced when the decision variables n is bigger. However,
 451 SPEA2-AHX can consistently outperform SPEA2-SBX on ZDT1, WFG1, DTLZ1 and UF1 with 10, 30, 50 decision variables. These
 452 experiments validate that the advantage of AHX over SBX is not affected by the dimensionality of MOPs.

453 5. Conclusion and future work

454 In this paper, an adaptive hybrid crossover operator HBX is designed, which is essentially a novel gene-level based
 455 crossover operator. Different from the existing hybrid crossover operators based on chromosome level, our AHX operator
 456 combines the local search ability of SBX and global search capability of DE from gene level, which jointly performs the ex-
 457 ploration and exploitation search. Due to the fact that the performance of HBX is high affected by the settings of P_1 and P_2
 458 during the evolutionary process, an adaptive parameter control approach is further designed for HBX to form AHX, which
 459 help to keep the balance between the exploitation and exploration search. To assess the performance of AHX, it is compared
 460 with two state-of-the-art crossover operators (SBX and DE) in the frameworks of NSGA-II, SPEA2, SMS-EMOA, and MOEA/D.
 461 Besides that, AHX is also compared with three recently proposed hybrid crossover operators (DEI, JGBL, and FRRMAB). The
 462 experimental results show that AHX is more effective than SBX, DE, DEI, JGBL and FRRMAB in solving various types of MOPs.

463 In our future work, the AHX operator will be further analyzed and enhanced to better solve many-objective optimization
 464 problems and constraint optimization problems. Moreover, other variation methods, such as Cauchy and Gaussian mutations,
 465 are investigated to hybridize with AHX or build a new hybrid crossover from gene level.

466 Acknowledgment

467 This work was supported by the National Natural Science Foundation of China under Grants 61402291 and 61170283,
 468 National High-Technology Research and Development Program ("863" Program) of China under Grant 2013AA01A212,
 469 Ministry of Education in the New Century Excellent Talents Support Program under Grant NCET-12-0649, Foundation for

470 Distinguished Young Talents in Higher Education of Guangdong under Grant 2014KQNCX129, Shenzhen Technology Plan
 471 under Grant JCYJ20140418095735608 and Natural Science Foundation of SZU under Grant 201531.

472 Reference

- [1] M. Antonelli, P. Ducange, F. Marcelloni, A fast and efficient multi-objective evolutionary learning scheme for fuzzy rule-based classifiers, *Inf. Sci.* 283 (2014) 36–54.
- [2] H.-G. Beyer, H.-P. Schwefel, Evolution strategies – A comprehensive introduction, *Nat. Comput.* 1 (2002) 3–52.
- [3] N. Beume, B. Naujoks, M. Emmerich, SMS-EMOA: Multiobjective selection based on dominated hypervolume, *Eur. J. Oper. Res.* 181 (2007) 1653–1669.
- [4] J.Y. Chen, Q.Z. Lin, Z. Ji, Chaos-based multiobjective immune algorithm with a fine-grained selection mechanism", *Soft Comput.* 15 (2011) 1273–1288.
- [5] G. Chen, C.P. Low, Z.H. Yang, Preserving and exploiting genetic diversity in evolutionary programming algorithms, *IEEE Trans. Evolut. Comput.* 13 (2009) 661–673.
- [6] Y.-C. Chuang, C.-T. Chen, C. Hwang, A real-coded genetic algorithm with a direction-based crossover operator, *Inf. Sci.* 305 (2015) 320–348.
- [7] M. Clerc, J. Kennedy, The particle swarm - explosion, stability, and convergence in a multidimensional complex space, *IEEE Trans. Evolut. Comput.* 6 (2002) 58–73.
- [8] L.Z. Cui, G.H. L, Q.Z. Lin, J.Y. Chen, N. Lu, Adaptive differential evolution algorithm with novel mutation strategies in multiple sub-populations, *Comput. Oper. Res.* (2015) <http://dx.doi.org/10.1016/j.cor.2015.09.006>.
- [9] S. Das, P.N. Suganthan, Differential Evolution: A survey of the state-of-the-art, *IEEE Trans. Evolut. Comput.* 15 (2011) 4–31.
- [10] K. Deb, R.B. Agrawal, Simulated binary crossover for continuous search space, *Complex Syst.* 9 (1995) 115–148.
- [11] K. Deb, A. Anand, D. Joshi, A computationally efficient evolutionary algorithm for real-parameter optimization, *Evolut. Comput.* 10 (2002) 371–395.
- [12] K. Deb, H. Jain, An evolutionary many-objective optimization algorithm using reference-point based non-dominated sorting approach, part I: Solving problems with box constraints, *IEEE Trans. Evolut. Comput.* 18 (4) 557–601.
- [13] K. Deb, A. Pratap, S. Agarwal, T. Meyarivan, A fast and elitist multiobjective genetic algorithm: NSGA-II, *IEEE Trans. Evolut. Comput.* 6 (2002) 182–197.
- [14] K. Deb, L. Thiele, M. Laumanns, E. Zitzler, Scalable multi-objective optimization test problems, in: Proceedings of the 2002 IEEE Congress on Evolutionary Computation (CEC), 1, Honolulu, HI, USA, 2002, pp. 825–830.
- [15] K. Deep, M. Thakur, A new crossover operator for real coded genetic algorithms, *Appl. Math. Comput.* 188 (2007) 895–911.
- [16] O.-B. Domingo, H.-M. Cesar, G.-P. Nicolas, CIXL2: A crossover operator for evolutionary algorithms based on population features, *J. Artif. Intell. Res.* 24 (2005) 1–48.
- [17] H. Dong, J. He, H. Huang, W. Hou, Evolutionary programming using a mixed mutation strategy, *Information Sciences* 177 (2007) 312–327.
- [18] M. Dorigo, L.M. Gambardella, Ant colony system: a cooperative learning approach to the traveling salesman problem, *IEEE Transactions on Evolutionary Computation* 1 (1997) 53–66.
- [19] J.J. Durillo, A.J. Nebro, E. Alba, The jMetal framework for multi-objective optimization: Design and architecture, in: Proceedings of the 2010 IEEE Congress on Evolutionary Computation (CEC), Barcelona, Spain, 2010, pp. 1–8.
- [20] S.M. Elsayed, R.A. Sarker, D.L. Essam, GA with a new multi-parent crossover for constrained optimization, in: Proceedings of the 2011 IEEE Congress on Evolutionary Computation (CEC), New Orleans, LA, 2011, pp. 857–864.
- [21] S.M. Elsayed, R.A. Sarker, D.L. Essam, A new genetic algorithm for solving optimization problems, *Engineering Applications of Artificial Intelligence* 27 (2014) 57–69.
- [22] L.J. Eshelman, J.D. Schaffer, Real-coded genetic algorithms and interval-schemata, in: Darrell L. Whitley (Ed.), *Proceedings of the Workshop on Foundations of Genetic Algorithms*, Vail, CO, USA, 1993, pp. 187–202.
- [23] C.M. Fonseca, P.J. Fleming, Genetic algorithms for multiobjective optimization: formulation discussion and generalization, in: S. Forrest (Ed.), *Proceedings of the Fifth International Conference on Genetic Algorithm*, 93, Urbana-Champaign, IL, USA, 1993, pp. 416–423.
- [24] D.E. Goldberg, *Genetic Algorithm in Search Optimization and Machine Learning*, Addison-Wesley, 1989.
- [25] S. Huband, L. Barone, L. While, P. Hingston, A scalable multi-objective test problem toolkit, in: C.A.C. Coello, A.H. Aguirre, E. Zitzler (Eds.), *Proceedings of Evolutionary Multi-Criterion Optimization*, Lecture Notes in Computer Science, 3410, Guanajuato, Mexico, 2005, pp. 280–295.
- [26] S.W. Jiang, Y.-S. Ong, J. Zhang, L. Feng, Consistencies and contradictions of performance metrics in multiobjective optimization, *IEEE Trans. Cybern.* 44 (2014) 2391–2404.
- [27] A.J. Jones, Genetic programming: on the programming of computers by means of natural selection – Koza, JR, *Nature* 363 (1993) pp. 222–222.
- [28] K. Kim, R.I. McKay, N.X. Hoai, Recursion-based biases in stochastic grammar model genetic programming, *IEEE Trans. Evolut. Comput.* doi: [10.1109/TEVC.2015.2425420](https://doi.org/10.1109/TEVC.2015.2425420).
- [29] J.D. Knowles, D.W. Corne, Approximating the nondominated front using the pareto archived evolution strategy, *Evolut. Comput.* 8 (2000) 149–172.
- [30] R. Koker, A genetic algorithm approach to a neural-network-based inverse kinematics solution of robotic manipulators based on error minimization, *Inform. Sci.* 222 (2013) 528–543.
- [31] M.Q. Li, S.X. Yang, K. Li, X.H. Liu, Evolutionary algorithms with segment-based search for multiobjective optimization problems, *IEEE Trans. Cybern.* 44 (2014) 1295–1313.
- [32] M.Q. Li, S.X. Yang, X.H. Liu, Shift-based density estimation for Pareto-based algorithms in many-objective optimization, *IEEE Trans. Evolut. Comput.* 18 (3) (2014) 348–365.
- [33] K. Li, A. Fialho, S. Kwong, Multi-objective differential evolution with adaptive control of parameters and operators, in: *Proceedings of the 5th International Conference on Learning and Intelligent Optimization (LION'11)*, Springer Verlag, LNCS, January 2011, pp. 473–487.
- [34] K. Li, A. Fialho, S. Kwong, Q.F. Zhang, Adaptive operator selection with bandits for multiobjective evolutionary algorithm based decomposition, *IEEE Trans. Evolut. Comput.* 19 (2014) 114–130.
- [35] K. Li, S. Kwong, J. Cao, M. Li, J. Zheng, R. Shan, Achieving balance between proximity and diversity in multi-objective evolutionary algorithm, *Inform. Sci.* 182 (1) (2012) 220–242.
- [36] K. Li, S. Kwong, K. Deb, A dual population paradigm for evolutionary multiobjective optimization, *Inform. Sci.* 309 (2015) 50–72.
- [37] K. Li, S. Kwong, K.-S. Tang, K.-F. Man, Learning paradigm based on jumping genes: a general framework for enhancing exploration in evolutionary multiobjective optimization, *Inform. Sci.* 226 (2013) 1–22.
- [38] K. Li, S. Kwong, Q.F. Zhang, K. Deb, Interrelationship-based selection for decomposition multiobjective optimization, doi: [10.1109/TCYB.2014.2365354](https://doi.org/10.1109/TCYB.2014.2365354).
- [39] K. Li, Q. Zhang, S. Kwong, M. Li, R. Wang, Stable matching-based selection in evolutionary multiobjective optimization, *IEEE Trans. Evolut. Comput.* 18 (6) (2014) 909–923.
- [40] H. Li, Q. Zhang, Multiobjective optimization problems with complicated Pareto sets, MOEA/D and NSGA-II, *IEEE Trans. Evolut. Comput.* 13 (2009) 284–302.
- [41] Q.Z. Lin, Q.L. Zhu, P.Z. Huang, J.Y. Chen, Z. Ming, J.P. Yu, A novel hybrid multi-objective immune algorithm with adaptive differential evolution, *Comput. Oper. Res.* 62 (2015) 95–111.
- [42] Q.Z. Lin, J.Y. Chen, A novel micro-population immune multiobjective optimization algorithm, *Comput. Oper. Res.* 40 (2013) 1590–1601.
- [43] I. Ono, H. Kita, S. Kobayashi, A robust real-coded genetic algorithm using the unimodal normal distribution crossover augmented by uniform crossover: effects of self-adaptation of crossover probabilities, in: W. Banzhaf, J. Daida, A.E. Eiben, M.H. Garzon, V. Honavar, M. Jakielka, R.E. Smith (Eds.), *Proceedings of the Genetic and Evolutionary Computation Conference*, 1, Orlando, FL, USA, 1999, pp. 496–503.
- [44] M. Pant, M. Ali, V.P. Singh, Differential evolution with parent centric crossover, in: *Proceedings of 2008 Second UKSIM European Symposium on Computer Modeling and Simulation (EMS)*, Liverpool, UK, 2008, pp. 141–146.

- 546 [45] Y.T. Qi, Z.T. Hou, M.L. Yin, H.L. Sun, J.B. Huang, An immune multi-objective optimization algorithm with differential evolution inspired recombination, Appl. Soft Comput. 29 (2015) 395–410.
- 547 [46] A.K. Qin, V.L. Huang, P.N. Suganthan, Differential evolution algorithm with strategy adaptation for global numerical optimization, IEEE Trans. Evolut. Comput. 13 (2009) 398–417.
- 548 [47] K.S.N. Ripon, S. Kwong, K.F. Man, A real-coding jumping gene genetic algorithm (RJGGA) for multiobjective optimization, Inform. Sci. 177 (2007) 632–654.
- 549 [48] M.D. Robles-Ortega, L. Ortega, F.R. Feito, A new approach to create textured urban models through genetic algorithms, Inform. Sci. 243 (2013) 1–19.
- 550 [49] D. Sanchez, P. Melin, O. Castillo, Optimization of modular granular neural networks using a hierarchical genetic algorithm based on the database complexity applied to human recognition, Inform. Sci. 309 (2015) 73–101.
- 551 [50] J.D. Schaffer, Multiple objective optimization with vector evaluated genetic algorithms, in: John J. Grefenstette (Ed.), Proceedings of the 1st International Conference on Genetic Algorithms, 1985, pp. 93–100.
- 552 [51] Y.L. Shang, R. Bouffanais, Influence of the number of topologically interacting neighbors on swarm dynamics, Sci. Rep. 4 (2014) 4184.
- 553 [52] Y.L. Shang, R. Bouffanais, Consensus reading in swarms ruled by a hybrid metric-topological distance, Eur. Phys. J. B 87 (12) (2014) 294.
- 554 [53] N. Sinha, R. Chakrabarti, P.K. Chattopadhyay, Evolutionary programming techniques for economic load dispatch, IEEE Trans. Evolut. Comput. 7 (2003) 83–94.
- 555 [54] H. Someya, Striking a mean- and parent-centric balance in real-valued crossover operators, IEEE Trans. Evolut. Comput. 17 (2013) 737–754.
- 556 [55] N. Srinivas, K. Deb, Multiobjective optimization using nondominated sorting in genetic algorithms, Evolut. Comput. 2 (1994) 221–248.
- 557 [56] R. Storn, K. Price, Differential evolution – a simple and efficient heuristic for global optimization over continuous spaces, J. Global Optim. 11 (1997) 341–359.
- 558 [57] L.X. Tang, X.P. Wang, A hybrid multiobjective evolutionary algorithm for multiobjective optimization problems, IEEE Trans. Evolut. Comput. 17 (2013) 45–45.
- 559 [58] M. Thakur, S.S. Meghwani, H. Jalota, A modified real coded genetic algorithm for constrained optimization, Appl. Math. Comput. 235 (2014) 292–317.
- 560 [59] S. Tsutsui, M. Yamamura, T. Higuchi, Multi-parent recombination with simplex crossover in real coded genetic algorithms, in: Proceedings of the Genetic and Evolutionary Computation Conference, I, Orlando, FL, USA, 1999, pp. 657–664.
- 561 [60] Z.K. Wang, Q.F. Zhang, A.M. Zhou, M.G. Gong, L.C. Jiao, Adaptive replacement strategies for MOEA/D, IEEE Trans. Cybern., doi: [10.1109/TCYB.2015.2403849](https://doi.org/10.1109/TCYB.2015.2403849).
- 562 [61] Y. Yoon, Y.-H. Kim, A. Moraglio, B.-R. Moon, A theoretical and empirical study on unbiased boundary-extended crossover for real-valued representation, Inform. Sci. 183 (2012) 48–65.
- 563 [62] H.-S. Yoon, B.-R. Moon, An empirical study on the synergy of multiple crossover operators, IEEE Trans. Evolut. Comput. 6 (2002) 212–223.
- 564 [63] X.D. Yu, J.B. Shao, H.B. Dong, On evolutionary strategy based on hybrid crossover operators, in: Proceedings of 2011 International Conference on Electronic and Mechanical Engineering and Information Technology (EMEIT), 5, Harbin, 2011, pp. 2355–2358.
- 565 [64] Q. Zhang, A. Zhou, S. Zhao, P.N. Suganthan, W. Liu, and S. Tiwari, Multiobjective optimization test instances for the CEC 2009 special session and competition, CES-487, 2008.
- 566 [65] Q.F. Zhang, H. Liu, MOEA/D: A multiobjective evolutionary algorithm based on decomposition, IEEE Trans. Evolut. Comput. 11 (2007) 712–731.
- 567 [66] Z.X. Zhu, S. Jia, S. He, Y.W. Sun, Z. Ji, L.L. Shen, Three-dimensional Gabor feature extraction for hyperspectral imagery classification using a memetic framework, Inform. Sci. 298 (2015) 274–287.
- 568 [67] E. Zitzler, K. Deb, L. Thiele, Comparison of multiobjective evolutionary algorithms: empirical results, Evolut. Comput. 8 (2000) 173–195.
- 569 [68] E. Zitzler, S. Knnli, Indicator-based selection in multiobjective search, in: Proceeding of the Eighth International Conference on Parallel Problem Solving from Nature (PPSN VIII), Springer, 2004, pp. 832–842.
- 570 [69] E. Zitzler, M. Laumanns, L. Thiele, SPEA2: Improving the strength Pareto evolutionary algorithm, Eidgenössische Technische Hochschule Zürich (ETH), Institut für Technische Informatik und Kommunikationsnetze (TIK), 2001.
- 571 [70] E. Zitzler, L. Thiele, Multiobjective evolutionary algorithms: a comparative case study and the strength pareto approach, IEEE Trans. Evolut. Comput. 3 (1999) 257–271.
- 572 [71] E. Zitzler, L. Thiele, M. Laumanns, C. Fonseca, V. da Fonseca, Performance assessment of multiobjective optimizers: an analysis and review, IEEE Trans. Evolut. Comput. 7 (2003) 117–132.